UNIVERSITÀ
DEGLI STUDI
DI PADOVA

PhD Thesis

Università degli Studi di Padova

Department of Surgery, Oncology and Gastroenterology

Ph.D. COURSE IN CLINICAL AND EXPERIMENTAL ONCOLOGY AND IMMUNOLOGY

SERIES XXXI

PATHOGENESIS OF NEUTROPENIA IN LARGE GRANULAR LYMPHOCYTE LEUKEMIA: IMMUNOPHENOTYPIC AND MOLECULAR CHARACTERIZATION OF NEUTROPENIC PATIENTS

The PhD Student Giulia Calabretto has been supported by a grant of Roche S.p.A., Italy

Coordinator: Prof. Paola Zanovello

Supervisor: Prof. Gianpietro Semenzato

Co-Supervisor: Dr. Renato Zambello

Dr. Antonella Teramo

Ph.D. Student: Giulia Calabretto

A journey of a thousand miles begins with a single step.

Lao Tzu

INDEX

ABBREVIATIONS

Ab	Antibody
Ag	Antigen
AICD	Activation-induced cell death
ANC	Absolute neutrophil count
ANKL	Aggressive NK leukemia
APC	Allophycocyanin
APC	Antigen-presenting cell
APS	Ammonium persulfate
Bcl-2	B-cell lymphoma-2
BSA	Bovine Serum Albumin
CD	Cluster of Differentiation
cDNA	Complementary DNA
CLPD-NK	Chronic lymphoproliferative disorder of natural killer cells
COSMIC	Catalogue of Somatic Mutations in Cancer
Ct	Threshold cycle
CTLs	Cytotoxic T Lymphocytes
DBD	DNA-binding domain
DC	Dendritic cells
ddNTPs	Dideoxynucleoside triphosphates
DISC	Death Inducing Signaling Complex
dNTPs	Deoxynucleotide triphosphates
EDTA	Ethylenediaminetetraacetic acid
ELISA	Enzyme-linked immunosorbent assay
FACS	Fluorescence Activated Cell Sorting
FasL	Fas Ligand
FCS	Fetal Calf Serum
FITC	Fluorescein isothiocyanate
FSC	Forward scatter
GAPDH	Glyceraldehyde 3-phosphate dehydrogenase
gp130	Glycoprotein 130
HCA	Hierarchical Clustering Analysis
HTLV	Human T-cell lymphotropic virus
IL-	Interleukin
JAK	Janus kinase
KIR	Killer immunoglobulin–like receptor

LGLL	Large Granular Lymphocyte leukemia
LGLs	Large Granular Lymphocytes
mAbs	Monoclonal antibodies
MHC	Major histocompatibility complex
miRNAs	MicroRNAs
mRNA	Messenger Ribonucleic Acid
NF-kB	Nuclear factor-κB
NK	Natural Killer
p-	Phospho-
PAGE	Poly-Acrylamide Gel electrophoresis
PBMCs	Peripheral blood mononuclear cells
PDGF	Platelet-derived growth factor
PE	Phycoerythrin
PE-Cy7	Phycoerythrin-Cyanine7
PI	Propidium iodide
PIAS	Protein inhibitor of activated STAT
PTPs	Protein tyrosine phosphatases
PVDF	Polyvinylidene difluoride
qRT-PCR	Quantitative Real-Time Polymerase Chain Reaction
RNA	Ribonucleic Acid
SDS	Sodium Dodecyl Sulfate
sFasL	Soluble-Fas Ligand
SH2	Src-homology 2
SOCS	Suppressor of cytokine signaling
SSC	Side scatter
STAT	Signal Transducer and Activator of Transcription
TAD	Transactivation domain
TBS	Tris buffered saline
TCR	T cell receptor
T-LGLL	T-Large Granular Lymphocytes leukemia
TYK2	Tyrosine kinase 2
VB	Variable β-
WHO	World Health Organization

ABSTRACT

Introduction

Large Granular Lymphocytes (LGLs) leukemia (LGLL) is a chronic lymphoproliferation of clonal cytotoxic LGLs, which can be divided in two different subsets, based on Cluster of Differentiation (CD)-3 expression: $CD3^-$ Natural Killer (NK) cells and $CD3^+$ ($CD8^+/CD4^-$ or $CD8^{-/dim}/CD4^+$) T-LGLs.

Leukemic LGLs are characterized by the up-regulation of several pro-survival signaling pathways. Among these, the most relevant is the JAK-STAT axis, whose constitutive activation is in part explained by somatic activating mutations in *STAT3* and *STAT5b*.

Neutropenia is the most frequent clinical manifestation. Despite being so common, its pathogenesis has not been well established yet, although high levels of soluble Fas Ligand (sFasL) were detected in serum of LGLL patients and supposed to trigger neutrophil's death.

Aims

This work aimed i) to describe the distinctive biological features of T-LGLs or NK cells of neutropenic LGLL patients; ii) to investigate the role of microRNAs in the regulation of FasL expression in leukemic LGLs.

Methods

LGLs were purified by FACSAriaIII cell sorter from peripheral blood mononuclear cells (PBMCs) of untreated LGLL patients and their immunophenotype was evaluated by Flow Cytometry. The screening of *STATs* mutations was performed by Sanger sequencing. PBMCs of patients were cultured *in vitro* and STAT3 transcriptional activity were inhibited or triggered with Stattic or IL-6, respectively. Transcriptional and protein expression levels were evaluated by Real Time-PCR, Western Blot (WB) assays and ELISA test.

High throughput and single miRNA analysis were carried out on purified T-LGLs by using the TaqMan® Human microRNA Array and Assays, respectively. Transfection with miR-146b mimic was performed using the Amaxa Nucleofactor and the Ingenio Electroporation Solution.

Results

We showed that leukemic T-LGLs of neutropenic patients were characterized by an immunophenotypic signature ($CD3^+/CD8^+/CD16^+/CD56^-$ phenotype) and by higher STAT3 activations, higher incidence of *STAT3* mutations and higher levels of sFasL, compared to T-LGLs of non-neutropenic patients. We also demonstrated that FasL transcription was mediated by STAT3 activation in T-LGLL patients.

The characterization of neutropenic CLPD-NK patients, instead, showed that they were characterized by $CD56^{-/dim}/CD16^{high}/CD57^-$ cytotoxic NK cells expansion. However, we observed a heterogeneous level of STAT3 activation and a heterogeneous expression of FasL in this subset of patients.

To investigate whether STAT3 could play its pathogenetic role through an altered expression of microRNAs, we studied miRNAs differentially expressed in patients characterized by neutropenia as compared to those with normal absolute neutrophil count (ANC). We showed that miR-146b expression, found down-regulated in neutropenic patients, was correlated with the ANC of T-LGLL patients.

To investigate miR-146b role in neutropenia development, we transfected purified $CD8^+$ T-LGLs with a miR-146b mimic. We showed that restoration of miR-146b led to a decrease of FasL mRNA, without changes in the FasL primary transcript, as compared to control. However, FasL was not identified among the putative miR-146b target genes, suggesting that miR-146b could regulate FasL expression indirectly. Therefore, we checked for genes involved in mRNA stability and we found that the defective miR-146b expression lead to increased transcriptional levels of the mRNA stabilizer HuR, that is required for FasL expression in T-lymphocytes. Consistently, by WB assays, we demonstrated that in T-LGLs of neutropenic patients HuR endogenous protein levels were higher than in T-LGLs of non-neutropenic ones. HuR-mediated FasL mRNA stabilization explained the increased FasL expression observed in neutropenic patients.

Conclusions

In this work we identify distinctive features of neutropenic LGLL patients, that could acquire relevance to correctly address the management of each patient, and we identify a miR-146b-FasL axis involved in neutropenia development in leukemic T-LGLs.

1. INTRODUCTION

1.1. Large Granular Lymphocytes

Large Granular Lymphocytes (LGLs) belong to the lymphoid lineage of hematopoietic cells and are mature post-thymic lymphocytes [1,2]. In normal adults, LGLs account for 5% to 15% of peripheral blood mononuclear cells (PBMCs) and their normal range is around 0.2-0.4 $x10^9$/L [3].

These cells are characterized by a distinct morphology (Figure 1): large size (15-18 μm), a round or reniform nucleus and an abundant cytoplasm with typical azurophilic granules, containing cytolytic components (such as perforin and granzymes B), which represent a cytotoxic equipment that allows LGLs to exert cytotoxic functions and, therefore, to play a central role in cell-mediated immune response [4].

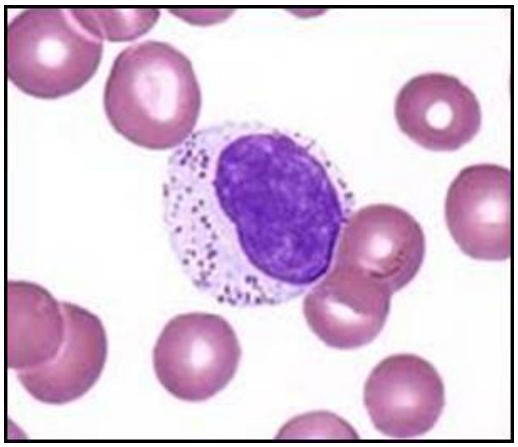

Figure 1.1. May-Grünwald-Giemsa staining of a large granular lymphocyte in peripheral blood: cytoplasmatic granules, in dark purple, are clearly visible.

LGLs can be divided into two different lineages, based on Cluster of Differentiation (CD)-3 expression: $CD3^-$ Natural Killer (NK) cells and $CD3^+$ Cytotoxic T Lymphocytes (CTLs) [1,2]. The large majority of LGLs (85%) belong to the NK cells subset, which represents the main component of innate immune system and mediates a major histocompatibility complex (MHC)-non-restricted cytotoxicity. The other subset of LGL population (accounting for the remaining 15%), is represented by CTLs, which are the main component of the adaptive immune system and express a receptor (named T cell receptor, TCR) that recognizes the antigen (Ag)-MHC molecule complex on antigen presenting cells (APC) surface, mediating a “MHC-restricted cytotoxicity” [5].

LGLs activation depends on antigen recognition, that leads to an approximately 50.000-fold proliferation of these cells. In physiological condition, upon antigen clearance, activated LGLs are then eliminated through a process known as activation-induced cell death (AICD), which represents an important mechanism for the maintenance of immune homeostasis.

An impairment of AICD process allows the maintenance of cytotoxic clones, since LGLs do not undergo apoptosis efficiently, leading to the development of a malignant condition, referred as Large Granular Lymphocyte Leukemia (LGLL) [6].

1.2. Large granular lymphocyte leukemia

1.2.1. Classification

Large granular lymphocyte leukemia embodies a spectrum of rare lymphoproliferative disorders sustained by the clonal expansion of CTLs or NK cells in peripheral blood, which can infiltrate different organs, including bone marrow, liver and spleen [7].

The 2016 World Health Organization (WHO) included this disease among mature T and Natural Killer cell neoplasms, dividing it into three categories, according to the cell lineage and the clinical course of the disease [8]. These are:

- T-Large Granular Lymphocyte leukemia (T-LGLL)
- Chronic Lymphoproliferative Disorder of NK cells (CLPD-NK)
- Aggressive NK leukemia (ANKL)

T-LGLL and CLPD-NK share an indolent and chronic nature, with similar clinical and biological features. The discovery of the same genetic lesions, both in leukemic T-LGLs and NK cells, suggests a common pathogenetic mechanism that contributed to unify these entities, despite they arise from different cell lineages [9]. In contrast, ANKL is characterized by a highly aggressive clinical behavior [10], therefore it has been suggested to be a separate clinicopathologic entity within NK cells lymphoproliferations

1.2.2. Epidemiology

LGL leukemia accounts for 2% to 5% of chronic lymphoproliferative disorders in North America and Europe and for 5% to 6% in Asia [11]. Recently, the incidence of LGLL has been published from two registries, including data from the two biggest retrospective series.

The Dutch registry reported 0.72 cases per 1 million individuals per year, whereas the American registry found 0.2 cases per 1 million individuals per year. Remarkably, its incidence does not differ between male and female [12].

LGLL is commonly diagnosed in elderly patients, with a median age of 66.5 at diagnosis. T-LGLL is the most frequent form of the disease, representing ~85% of the cases, whereas CLPD-NK is estimated at <10% of cases [5]. ANKL, that is mainly seen in Asia, comprises <5% of the LGL disorders. It affects younger patients and is associated with Epstein-Barr virus infection [13].

1.2.3. Diagnosis

LGLL diagnosis requires evidence of a chronic expansion of clonal LGLs, harboring a constitutive mature post-thymic phenotype, associated with an appropriate clinical context [1].

First of all, diagnosis is based on the documentation of an increased numbers of circulating LGLs. Historically, the threshold of 2×10^9/L was mandatory. However, numerous patients present lower clonal expansion of LGLs, typically associated with cytopenias or autoimmune conditions. Thus, a threshold of 0.5×10^9/L is now generally accepted. Notably, the cytology of clonal LGLs is not different compared to their normal counterpart [12].

Immunophenotype analyses have revealed that NK cells show a TCRαβ$^-$/sCD3$^-$/CD3ε$^+$/ /CD4$^-$/CD8$^+$/CD16$^+$/CD56$^+$/CD57$^\pm$ phenotype. These cells represent a heterogeneous population that can be divided into two main subsets, based on the different density of expression of CD16 and CD56: CD56^{dim}/CD16^{bright}, which represent about 90% of NK cells in peripheral blood, and CD56^{bright}/CD16$^{dim/neg}$ [14].

Leukemic T-LGLs, instead, show a terminal effector memory phenotype, characterized by CD3$^+$/CD4$^-$/CD5^{dim}/CD8$^+$/CD27$^-$/CD28$^-$/CD57$^\pm$/CD62L^{dim}/CD45RA$^+$ expression[11]; in addition, T-LGLs can also express cytotoxic NK cell markers and receptor, including CD16, CD56, killer immunoglobulin–like receptor (KIR) and C-type lectin receptor, as the CD94/NKG2 heterodimer. A rare subset of leukemic T-LGLs can also be CD4$^+$, with or without coexpression of CD8. CD4 and CD8 expression, indeed, identifies lineage with different functions.

The CD4 antigen is characteristic of T-helper lymphocytes, which represent a regulatory lymphocyte lineage, while the CD8 antigen is typical of cytotoxic T lymphocytes, which have effector functions [15]. Despite the expression of CD4, these cells can be classified as cytotoxic T lymphocytes.

The clonal nature of T-LGLs expansion can be established through the detection of TCR rearrangement. T-LGLs typically harbor an $\alpha\beta^+$ TCR a few, uncommon, T-LGLs can express a $\gamma\delta^+$ TCR, but these cells are rarely detected. Clonality can also be assessed by flow cytometry, through the demonstration of a predominant TCR Variable β-chain (Vβ) family expression.

To assess the clonality of NK cells, which instead do not express TCR, restricted expression of isoforms of killer immunoglobulin–like receptors has been used as a surrogate marker for clonal expansion [16].

1.2.4. Differential Diagnosis

Many conditions can lead to the development of reactive LGLs proliferation, including splenectomy, solid organ or bone marrow graft, viral infections (human immunodeficiency virus, Epstein-Barr virus, cytomegalovirus), solid tumor and non-Hodgkin lymphoma. In these cases, LGLs proliferations are typically poly- or oligoclonal, lasting only several months and are not responsible for cytopenias development. In difficult cases, bone marrow biopsy could be useful to define diagnosis, because in reactive LGL proliferation, bone marrow infiltration is generally absent [12].

1.2.5. Clinical manifestations

Approximately one-third of patients are asymptomatic at diagnosis, whereas two-thirds of patients will become symptomatic during the course of the disease. Clinical manifestations include mainly cytopenias and autoimmune disorders [17,18].

Neutropenia represents the most frequent clinical manifestation observed in LGLL patients: almost 85% of patients experience neutropenia and about 45% of them develop severe neutropenia. Therefore, initial presentation is often dominated by recurrent infections related to neutropenia, even if some neutropenic patients remained asymptomatic. Infections secondary to chronic neutropenia affect 15% to 39% of patients, involving primarily skin, oropharynx, and the perirectal area.

Severe septic complications may occur in about 5% to 10% of patients, representing the primary cause of related death [19,20].

Among cytopenias, transfusion-dependent anemia affects between 6% and 22% of patients according to series, and pure red cell aplasia occurs in 8% to 19% of cases. Thrombocytopenia, instead, is less severe and described in fewer than 20% of cases.

A quarter of patients harbor splenomegaly, although hepatomegaly or lymphadenopathy is rarely observed.

B symptoms and fatigue are rare and they are observed in only 20% to 30% of cases [12].

Remarkably, LGLL is commonly associated with autoimmune diseases, reported in about 15% to 40% of patients. Rheumatoid arthritis is the most frequent and is present in about 15% of the cases. Autoimmune cytopenias are reported among 5% to 10% of patients. Systemic lupus erythematosus, Sjögren's syndrome, autoimmune thyroid disorders, coagulopathy, and inclusion body myositis have occasionally been reported. Vasculitis with cryoglobulinemia was also reported. Moreover, cases of pulmonary artery hypertension considered as a vasculopathy with endothelial dysfunction were reported to be associated with LGLL [21,22].

Serum protein electrophoresis usually shows polyclonal hypergammaglobulinemia as a result of increased immunoglobulin G and/or A subclasses. Hypogammaglobulinemia is seen in 5% to 10% of patients. Defects in downregulation of immunoglobulin secretion in LGL leukemia could partly explain the development of autoantibodies and clonal B-cell malignancies observed in this disease, monoclonal gammopathy of undetermined significance being the most frequent (10%–20%).

Furthermore, chronic lymphoid leukemia, follicular lymphoma, mantle cell lymphoma and other neoplasia are also reported to be associated with LGLL [11,12].

1.3. Neutropenia

Neutropenia is a reduction in the absolute neutrophils count (ANC) in the blood circulation and represents the most frequent cytopenia observed in LGLL patients.

Neutropenia may be distinguished as:

- mild neutropenia, with an ANC of 1.0-1.5 $x10^9$/L;
- moderate neutropenia, with an ANC of 0.5-1.0 $x10^9$/L;
- severe neutropenia, with an ANC lower than 0.5 $x10^9$/L.

The mechanism of neutropenia development in LGLL patients is not well understood and its pathogenesis is reported to be multifactorial, including both humoral and cytotoxic mechanisms [17,23]. Any acquired neutropenia may result from reduced and/or ineffective granulopoiesis and/or shortened neutrophil survival

An alternative mechanism to account for neutropenia might be the impairment of granulopoiesis due to bone marrow (BM) infiltration by pathological LGLs [24,25]. However, in LGLL patients, it does not appear to be the major cause, as the analysis of the BM biopsy and aspirate in these patients usually reveals mild hypercellularity, whereas granulocytic progenitors are most often decreased and demonstrate a left-shifted myeloid maturation. In addition, neutropenia is more common and more severe than anemia and thrombocytopenia. This observation supports the hypothesis that neutropenia could be due mainly to peripheral destruction.

Consistently with this assumption, neutropenia may be due to splenic sequestration or destruction of neutrophils. However, although splenomegaly is documented in 20–50% of LGLL patients, there are no data to support a major pathogenetic role for hypersplenism in LGLs-associated neutropenia.

LGLs isolated from healthy individuals were reported to suppress the growth of BM granulocyte–macrophage colony-forming cells. Nevertheless, coculture of leukemic T-LGLs with BM derived from normal donors or with autologous BM, did not resulted in a significant inhibition of granulocyte– macrophage colony-forming cells.

Several studies have also indicated the presence of antineutrophil antibodies in the sera of some neutropenic patients diagnosed with LGLL. However, in most of these cases, the possibility that the detected antibodies were anti-HLA antibodies, rather than true neutrophil autoantibodies, was not properly addressed. In addition, circulating immune complexes, which are more often present in the serum of LGLL patients, may limit the ability of tests to identify specific neutrophil autoantibodies. In a study, undertaken in five patients with T-LGL leukemia, the authors found low levels of immune complexes in only one patient and no definitive neutrophil autoantibodies in the remaining four patients. Collectively, immune-mediated destruction of neutrophils, via granulocyte antibodies and immune complexes, cannot be excluded [26,27].

Among the cytotoxic mechanisms accounting for neutropenia development, also abnormal expression of KIR has been considered, since it has been demonstrated to be associated with pure cell aplasia [28].

However, the most supported mechanism accounting for neutropenia development is myeloid progenitor and neutrophil destruction via Fas-mediated apoptosis. Leukemic T-LGLs, indeed, constitutively express FasL on their surface, in contrast to normal CTLs, in which FasL expression is consequent to their activation. Engagement of the death receptor Fas on the surface of target cells by FasL triggers apoptotic pathways [29].

It has been established that mature neutrophils constitutively express Fas at higher levels than monocytes and eosinophils [30]. In addition, neutrophils have been shown to be more sensitive to Fas-mediated apoptotic cell death than monocytes or eosinophils. Although FasL is constitutively expressed on the surface of T-LGL leukemic cells, it can be shed in a soluble form (sFasL) by the action of metalloproteinases. Consistently, sFasL has been found markedly elevated in the sera of LGLL patients. Furthermore, sera from patients with T-LGL leukemia with elevated sFasL were shown to induce apoptosis in normal neutrophils in vitro and, remarkably, the clinical response to therapy for neutropenia in those patients was associated with a reduction in sFasL levels [31].

Despite Fas is normally expressed by various hematopoietic cell subsets, normal CD34+ hematopoietic progenitor cells do not express this antigen under steady-state conditions. However, when $CD34^+$ cells are cultured in the presence of TNF-α and/or IFN-γ, they show increased expression of functional Fas. Furthermore, $CD34^+$ cells from patients with aplastic anemia, who have consistently elevated levels of TNF-α and IFN-γ, upregulate Fas expression on $CD34^+$ hematopoietic progenitors. Interestingly, lymphocytes from some patients with T-LGL leukemia spontaneously secrete IFN-γ and can also be induced to produce TNF-α. Based on these observations, it has been proposed that in T-LGL leukemia, TNF-α and IFN-γ, together with the overproduction of FasL, may induce Fas-mediated apoptosis of granulocytic progenitor. However, it has nott been clarified why the effects of these cytokines would concern only a specific lineage in T-LGL, whereas in aplastic anemia a broader suppression of hematopoietic cell subsets would occur [32], [33].

1.4. Pathogenesis

1.4.1. Etiology

The etiology of LGLL still remains matter of debate, due to the fact that no single, specific agent but a series of events have a role in triggering LGLs proliferation [34]. Some reports strongly support the role of chronic antigenic stimulation by exogenous antigens, such as human T-cell lymphotropic virus (HTLV) or putative endogenous autoantigens as the initial stimulus inducing the activation and then the clonal expansion of effector LGLs [35].

The exact role of retroviral infection as etiologic agent has not been entirely established. It has been described that most patients with LGLL are not infected with prototypical HTLV, however they showed serum reactivity against a small peptide derived from the HTLV-I envelope protein p21e [36].

1.4.2. Pathogenesis

LGLL pathogenesis is still incompletely understood. The first step of LGLs proliferation is related to the chronic antigenic stimulation, which lead to a polyclonal expansion. Later, clonal proliferation and LGLs survival are sustained by interleukin (IL)–15 and IL-2 proinflammatory cytokines and by platelet-derived growth factor (PDGF) (Figure 1.2).

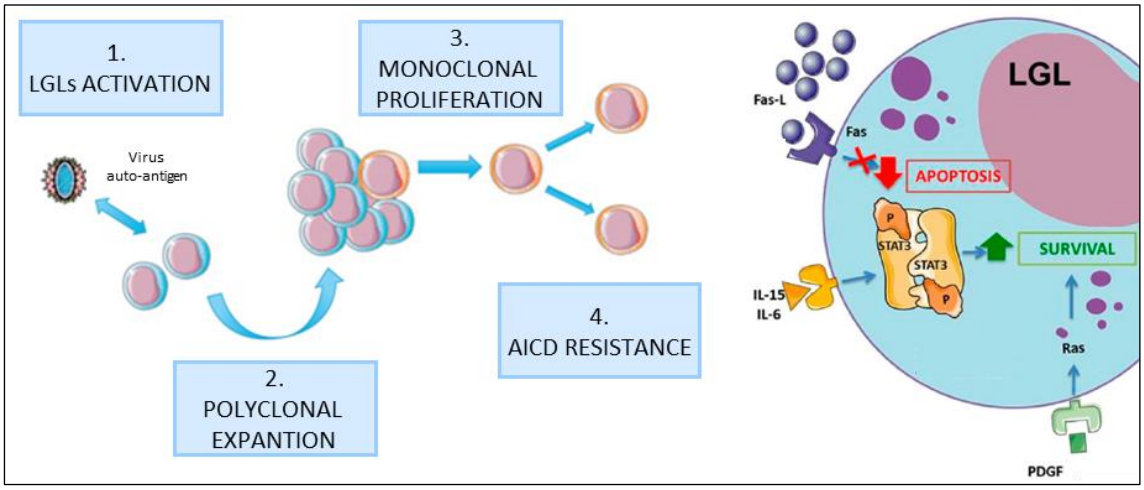

Figure 1.2. LGLL pathogenetic hypothesis.

In addition, gene-profiling analysis has shown that leukemic LGLs are characterized by an upregulation of proapoptotic genes, whereas anti-apoptotic genes are reported to be downregulated.

A work of our lab has also shown a possible role for dendritic cells (DC) in the pathogenesis of LGLL. These cells belong to the antigen-presenting cell (APC) family, characterized by the ability to recognize antigens and later to present the same antigens and adhesion molecules on their surface to T cells, inducing their activation. DCs can be involved in LGLs proliferation after the recognition of a specific antigen that maintains proliferation by releasing cytokines like IL-2, IL-15 and IL-18. Immunohistochemical analysis performed on osteo-medullary biopsies of T-LGLL patients have shown the presence of direct contact between LGL and DC, in contrast to healthy controls, in which cells have a random distribution. Therefore, it has been hypothesized that the medullary environment represents the place where pathological proliferation starts and thus, DCs representing viral infection target cells.

Another possible mechanism implicated in the inhibition of apoptosis is due to the resistance to Fas-mediated apoptosis. Leukemic LGLs, indeed, despite abundant and constitutive expression of Fas and FasL on thei surface, are resistant to Fas-mediated apoptosis. Interestingly, this cannot be attributed to dysfunctional Fas/FasL mutations. On the other hand, sera from LGL leukemia patients have been shown to contain elevated levels of a soluble form of Fas (sFas), which may act as a decoy receptor for FasL, thereby resulting in the Fas-resistant phenotype of leukemic LGLs. This resistance can also be partly attributed to impaired death-inducing signaling complex (DISC) formation. Normally, DISC assembly is the immediate downstream event of Fas–FasL cross-linking and is a prerequisite for Fas-mediated apoptosis. However, in leukemic LGLs, the overexpression of the DISC inhibitory protein FLIP is thought to impair DISC formation and thus prevent Fas-mediated apoptosis.

Taken together, these mechanisms may account for the resistance of LGL cells to AICD mechanism.

1.4.3. Dysregulated pathway

A constitutive activation of different signaling pathways has been demonstrated in LGLs of patients, and significantly contribute to the escape of these cells from activation-induced cell death (Figure 1.3) [37,38].

These include:

- JAK/STAT;
- Fas/Fas Ligand
- Nuclear factor (NF)-κB;
- Ras/Mek/Erk;
- PI3K/Akt;
- Sphingolipid Rheostat.

Among these, one of the most relevant is the JAK/STAT axis.

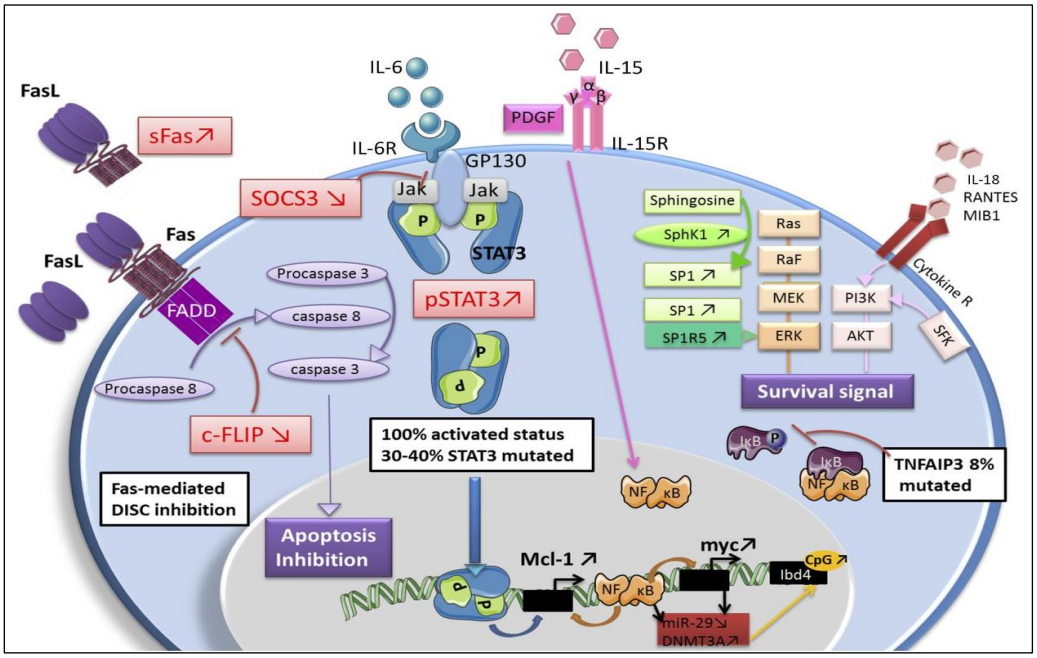

Figure 1.3. Deregulated signaling pathways in leukemic LGLs.

1.5. JAK-STAT pathway

1.5.1. Regulation

Janus kinase-Signal Transducer and Activator of Transcription (JAK-STAT) pathway is a fundamental signaling cascade that transduces multiple signals from transmembrane receptors to the nucleus. The pathway is activated by the binding of a cytokine or a growth factor to its respective transmembrane receptors.

Ligand binding induces the receptor dimerization/oligomerization. This leads to the activation of receptor-associated tyrosine kinases JAKs, which comprise four members: JAK1, JAK2, JAK3 and tyrosine kinase 2 (TYK2).

JAKs activation leads to their cross-phosphorylation and to tyrosine phosphorylation of the cytoplasmic regions of the receptor with which they are associated.

As a result, docking sites for downstream effector STAT proteins, containing phosphotyrosine recognition domains, are generated. STAT monomers are then recruited to the phosphorylated receptors, undergo tyrosine phosphorylation themselves and dimerize. The STATs dimers then translocate from the cytoplasm into the nucleus, where they regulate fundamental biological processes, by activating the expression of genes involved in cell differentiation, proliferation, inflammation and apoptosis (Figure 1.4) [39].

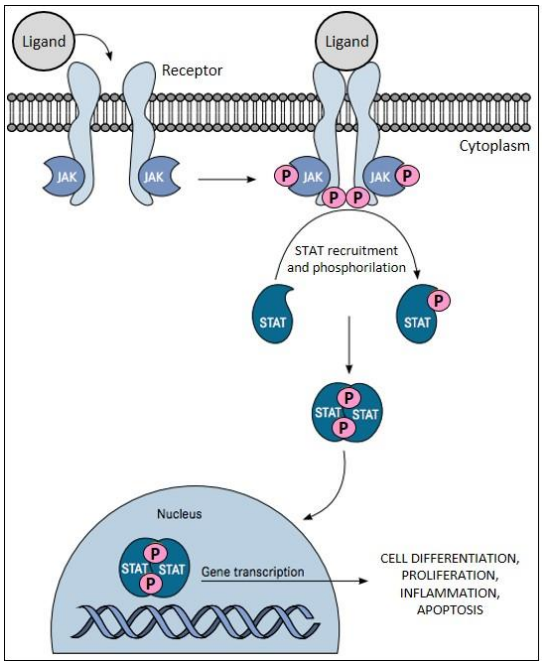

Figure 1.4. JAK/STAT signaling pathway.

STAT proteins bind to tens of thousands of different sites in the genome, thereby they regulate the transcription of thousands of protein-coding genes, including oncogenes and tumor suppressors. Therefore, activity of the JAK-STAT pathway is finely regulated on multiple levels, to ensure suppression of signaling in the absence of cytokine recognition, but also to allow rapid, transient activation upon stimulation. This regulation is crucial, since a persistent activation of STAT proteins or an aberrant signaling might result in malignancies, autoimmune or inflammatory diseases.

The JAK–STAT signaling can be regulated through different mechanisms, including the suppressor of cytokine signaling (SOCS) proteins and the protein inhibitor of activated STAT (PIAS) family, as well as various protein tyrosine phosphatases (PTPs) [40].

1.5.2. STATs proteins

The mammalian family of STATs proteins consists of 7 members: STAT1, STAT2, STAT3, STAT4, STAT5a, STAT5b and STAT6.

The STAT proteins share structurally and functionally conserved domains, including: a N-terminal domain, a coiled-coil domain, a DNA-binding domain (DBD), a linker domain, a Src-homology 2 (SH2) domain and a C-terminal transactivation domain (TAD) (Figure 1.5). Among these, the SH2 domain mediates homo and heterodimer formation of STATs monomers [41].

Figure 1.5. Schematic representations of Signal transducer and activator of transcription (STAT) domains.

Among the seven STATs members, STAT3 and STAT5b are the most significant in cancer development, whereas the other appear to have more limited roles in oncogenesis. Consistently, STAT3 and STAT5b constitutive activation have been found to be associated with initiation and progression of various cancers. The constitutive activation of these proteins can be the result of different aberrant mechanisms: increased upstream stimulation of kinases, lack of negative regulation or somatic activating mutations. Consistently, based on data collected from the Catalogue of Somatic Mutations In Cancer (COSMIC), STAT3 results the most frequently mutated gene from the STAT family in hematopoietic neoplasm, followed by STAT5b [42].

1.5.3. STAT3 and STAT5b

The *STAT*3, *STAT5a*, and *STAT5b* genes are located on the long arm of chromosome 17, in adjacent regions (17q11.2).

STAT3 exists in two major isoforms: full-length STAT3α is 770 amino acids long, while the shorter form STAT3β, arising from an alternative mRNA-splice site at exon 23, gives origin to a protein in which the last 55 C-terminal amino acid residues are replaced by 7 other residues. Thus, STAT3β lacks the TAD domain and seems to have specific functions of its own, as it can prevent the embryonic lethality of STAT3α-null mice and activate a set of STAT3 target genes.

STAT3 is essential for development, and total STAT3 ablation leads to early embryonic lethality in mice [43]. Targeted disruption of STAT3 function in mouse T-cells results in impaired IL-6-mediated survival and reduced proliferative response when stimulated with IL-2 [44], [45].

STAT5a and STAT5b, instead, are separate genes. The coded proteins are 794 and 787 amino acids long, respectively, and are over 90% identical at cDNA and protein level. STAT5b is required for the development and normal function of lymphocytes.

Recent studies have shown that total *STAT5a/b* deletion in mice leads to high perinatal lethality, severe combined immunodeficiency, and a lack of lymphoid cells, further emphasizing the pleiotropic role of STAT5 proteins in immune system function [46,47].

Stat5a-/- mice display impaired mammary gland development, whereas *Stat5b-/-* mice display impaired pituitary growth hormone production and consequently diminished body growth. Considering the function of the immune system, bone marrow derived macrophages of *Stat5a-/-* mice exhibit defective GM-CSF–induced proliferation and gene expression in addition to other immunological defects, including a reduced number of T and NK cells *in vivo*. The T-cell defect is associated with diminished IL-2–mediated signaling. Stat5b-/- mice present with a diminished absolute number of NK cells and a maturation block in bone marrow; the NK cell numbers are lower than in Stat5a-/- mice and NK-cell proliferation and cytolytic activity to IL-2 and IL-15 stimulation is poor. The T-cell defect is associated with diminished IL-2–mediated signaling [48].

1.5.4. STAT3 in LGLL

STAT3 activation represents a hallmark of leukemic LGLs. Epling-Burnette et al., indeed, reported that leukemic LGLs constitutively express high levels of activated STAT3, compared to LGLs of healthy individuals [49].

Several studies report aberrant mechanisms leading to STAT3 activation, including the presence of somatic activating mutations. Consistently, several *STAT3* mutational hotspots have been detected in 30%-40% of T-LGL leukemia patients and in one-third of the CLPD-NK patients (Figure 1.6) [9,50].

The most frequent are Y640F and D661Y, located in the SH2 domain, which promote the dimerization, phosphorylation and localization in the nucleus of STAT3 proteins.

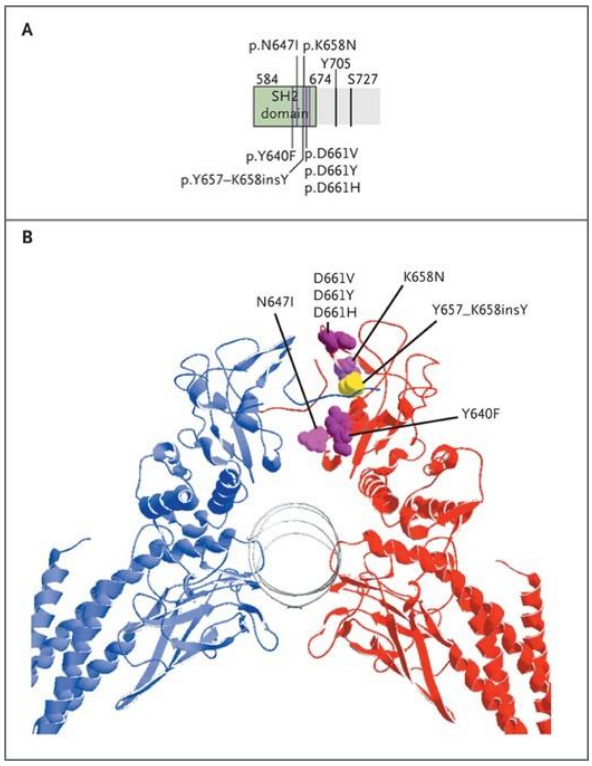

Figure 1.6. Locations of STAT3 mutations and crystal structure of STAT3 homodimer.

Anyway, in a study by Andersson et al, activating STAT3 mutations were also detected in the coiled-coil and DBD domains. Phenotypically, no difference was observed between patients with somatic mutations in the SH2 domain compared to those with mutations in the DBD and in the coiled-coil domain [51].

STAT3 mutations represent the most distinctive genetic lesions described in this disease. Despite their high mutational frequency, some studies question the role of these genetic lesions as the driver mutations in LGLL. For instance, it was demonstrated that expression of the STAT3 mutations were insufficient to induce LGL leukemia in mice models, and it was suggested that STAT3 mutations do not play a causal role in development of T-LGL leukemia and that additional gene mutations and deregulation of other signaling pathways, in association with STAT3 mutations, may cause T-LGL leukemia [52].

STAT3 activation is also promoted by not-mutational mechanisms. Teramo A. et al., demonstrated that IL-6, which is the most important STAT3 activator, was highly released by LGLs-depleted PBMCs of patients, compared with healthy controls, suggesting that STAT3 activation may result from the persistent stimulation of this cytokine [53].

In addition, they provide evidence of a down-modulation of SOCS3 in leukemic LGLs, due to an epigenetic modulation, that leads to the lack of the physiological negative feedback mechanism controlling STAT3 activation [53].

These two pathological mechanisms cooperate to maintain STAT3 activation even in STAT3 wild-type patients. Consistently, different studies have shown that almost all T-LGLL patients are characterized by the activation of the STAT3 pathway, even without somatic mutations in the STAT3 gene. Andersson E. et Al. performed exome sequencing on 3 *STAT3*-mutation negative T-LGLL patients. They found an activated STAT3 pathway, by RNA expression and phospho STAT3 analysis, indicating that LGLL patients are characterized by the activation of STAT3 responsive genes even without the presence of somatic mutations in *STAT3* gene [54].

1.5.5. STAT5b in LGLL

STAT5b mutations (Y665F and N642H) were initially found in a smaller subset (2%) of T-LGLL patients, reported to have a distinctive immunophenotype ($CD3^+/CD8^+/CD56^+$) and a clinically aggressive disease, with a poor prognosis [54]. Then, in a study by Andersson et al, *STAT5b* mutations were detected also in 55% of $CD4^+$ T-LGLL patients. Based on these data, the authors concluded that *STAT5b* mutations are more unique, but not exclusive, for the $CD4^+$ phenotype than for the $CD8^+$ phenotype. Clinically, *STAT5b* mutated $CD4^+$ T-LGLL patients show an indolent and asymptomatic disease, in contrast to the previous assumptions regarding the clinically aggressive disease observed in $CD8^+$ T-LGLL patients harboring these genetic lesions [55].

1.6. Treatment

T-LGLL and CLPD-NK- share the same treatment options. Indications for treatment include moderate or severe neutropenia associated with recurrent infections, symptomatic or transfusion-dependent anemia, and associated autoimmune conditions requiring therapy.

Guidelines for first line treatment in LGLL have not been established due to the lack of large prospective trials. First-line therapy relies on single immunosuppressive oral agents: methothrexate (MTX) (10 mg/m^2 per week), cyclophosphamide (100 mg/d), or ciclosporin A (3 mg/kg per day) [12].

Treatment efficiency is reported by several retrospective series, but only a few prospective trials are available. First-line therapy results are detailed in Table 1.1 (only series including more than 10 patients are reported).

Therapy	Type of Study	Number of Patients	ORR, % (No. of Patients)	CR (No. of Patients)
Methotrexate				
Sanikommu et al (2018)[8]	Retrospective	34	44% (15)	
Bareau et al (2010)[7]	Retrospective	36	44% (16)	14% (5)
Loughran et al (1994)[52]	Prospective	10	60% (6)	50% (5)
Loughran et al (2015)[45]	Prospective	54	38% (21)	5% (3)
Cyclophosphamide				
Sanikommu et al (2018)[8]	Retrospective	22	47% (10)	
Moignet et al (2014)[53]	Retrospective	45	72% (32)	47% (21)
Poullot et al (2014)[54]	Retrospective	13	69% (9)	46% (6)
Dhodapkar et al (1994)[55]	Retrospective	16	63% (10)	38% (6)
Cyclosporine				
Sanikommu et al (2018)[8]	Retrospective	44	45% (20)	
Osuji et al (2006)[56]	Retrospective	14	92% (13)	

Abbreviations: CR, complete responses; ORR, overall response rate.
Only series including more than 10 patients are reported.

Table 1.1. First-line therapy results.

MTX and cyclophosphamide are the main immunosuppressive agents used for LGLL treatment. Overall response rates, however, ranges from 35% to 65%, and relapses frequently occur, due to the persistence of leukemic clone.

Deep sequencing analyses of residuals LGLs clones reveals that cyclophosphamide may eradicate leukemic cells, providing durable response, whereas MTX and ciclosporin A treatment are associated with the persistence of leukemic clones. These results remain to be validated in prospective trials.

An important randomized trial (NCT01976182) investigating first-line MTX versus cyclophosphamide is ongoing in France and will hopefully determine the best choice of initial therapy in this disease [12]. Of interest was that STAT3 mutations at Y640F seemed to predict a response to methotrexate since all patients with this mutation better responded to this immunosuppressive agent [56].

2. AIM

Large Granular Lymphocytes (LGLs) leukemia (LGLL) is a chronic lymphoproliferation of clonal T-LGLs or Natural Killer (NK) cells. Leukemic LGLs are characterized by the constitutive activation of JAK/STAT pathway, which is in part explained by the high frequency of somatic activating mutations in *STAT3* and *STAT5b* genes.

Neutropenia is the most frequent clinical manifestation observed in LGLL patients and represents a negative prognostic factor, since it might lead to recurrent infections. The mechanism leading to neutropenia development is still elusive, although literature data suggest that its pathogenesis could be multifactorial, comprising both humoral and cytotoxic mechanisms. One of most relevant hypotheses is the deregulated expression of Fas Ligand (FasL) by leukemic LGLs, since normal neutrophil survival is partly regulated by the Fas-FasL apoptotic system. Consistently, high levels of soluble FasL (s-FasL) have been detected in LGLL patients' serum, likely triggering neutrophil apoptosis.

The aim of this project were: i) to characterize neutropenic LGLL patients, identifying distinctive biological features that might become both a prognostic tool to recognize this high-risk category of patients and new potential therapeutic targets for neutropenia treatment; ii) to elucidate the molecular mechanism of neutropenia development, investigating the role of microRNAs, regarded as important gene expression regulators[57], often involved in the pathogenesis of cancer, in the regulation of sFasL expression. Therefore, considering the biological heterogeneity of the disease, we evaluated:

- the immunophenotype of the leukemic clone, by flow cytometer analysis;
- STAT3 activation level, by western blot assays;
- *STAT3* and *STAT5b* mutational status, by Sanger sequencing;
- FasL transcriptional and protein levels, by Real Time-PCR and ELISA test;
- Regulatory mechanism of FasL expression, by *in-vitro* inhibition and induction of STAT3 transcriptional activity;
- miRNA pattern of expression in LGLs of neutropenic patients, compared to patients with normal neutrophil count, by a high throughput and single miRNA analysis.

3. MATERIALS AND METHODS

3.1. Samples and ethical permission

Samples were collected from 100 LGLL patients and 10 healthy donors. Patients referred to the Hematology and Clinical Immunology Division at the University of Padua and the diagnosis of LGLL was based on the WHO 2016 criteria. At the time of the study, none of them had received treatments.

For some experiments, the Jurkat cell line was used. It is an immortalized T lymphocyte cell line that was established in the late 1970s from the peripheral blood of a 14-year-old boy with T cell leukemia.

All studies were conducted in accordance to the principles of the Helsinki declaration and written informed consents were obtained from all enrolled patients and healthy donors.

3.2. Mononuclear cells separation

Peripheral blood mononuclear cells (PBMCs) of patients and healthy donors were isolated from EDTA-treated peripheral blood by density gradient centrifugation with Ficoll-Paque™ PLUS (GE Healthcare Bio-Science; Pittsburgh, USA). This reagent is a sterile density gradient media for isolating mononuclear cells from human peripheral blood, using a centrifugation procedure based on the method developed by Bøyum. Ficoll-Paque™ PLUS was slowly added at the bottom of the tube in which peripheral blood was collected, up to ½ of the total blood volume. The tube was then centrifuged at 2200 rpm for 20 minutes. A stratification of different components was produced, obtaining plasma, lymphocytes, monocytes, platelets, Ficoll-Paque™ PLUS, granulocytes and erythrocytes (Figure 3.1).

Red blood cells are efficiently aggregated by this agent at room temperature and collect as a pellet at the bottom of the tube. The layer immediately above the erythrocytes contains granulocytes. Lymphocytes, monocytes, and platelets, instead, are not dense enough to penetrate into the ficoll layer. Therefore, these cells collect as a concentrated band at the interface between plasma and the Ficoll-Paque™ PLUS and can be recovered with high yield in a small volume.

PBMCs are then subsequently washed and pelleted to removes platelets, any contaminating ficoll and plasma. The resulting cell suspension contains lymphocytes and monocytes and is suitable for further studies.

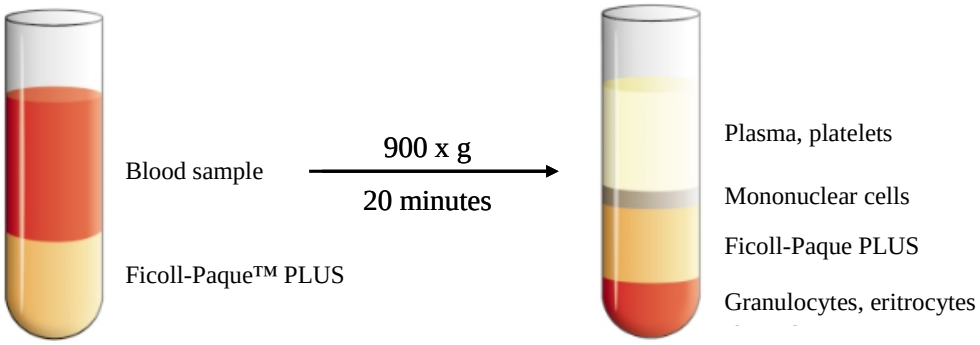

Figure 3.1. Schematic representation of stratification of different components obtained by density gradient centrifugation with Ficoll-Paque™ PLUS.

3.3. LGLs purification

Leukemic $CD57^+$ LGLs were purified from PBMCs of patients either by MACS® separation or by sorting with the FACSAria III cell sorter (BD Biosciences, San Jose CA, USA).
The normal counterpart of pathological T-LGLs, used as control and represented by $CD3^+CD8^+CD57^+$ lymphocytes, was sorted from PBMCs of healthy donors.

3.3.1. MACS® separation

$CD57^+$ LGLs were magnetically labeled with MACS® MicroBeads, conjugated to monoclonal anti-human CD57 antibodies (isotype: mouse IgM) (Miltenyi Biotec, Auburn, CA) and separated in a MACS® column, placed in a MACS® Separator. MACS® MicroBeads are 50-nm superparamagnetic particles, conjugated to highly specific antibodies against a specific cell surface antigen. Thanks to their small size, the beads do not activate cells, neither have to be removed for any downstream application. MACS® Column contain a matrix composed of ferromagnetic spheres covered with a cell-friendly coating. When the column is placed in a MACS® Separator, the spheres amplify the magnetic field by 10,000-fold, thus inducing a strong magnetic force within the column. The separation is based on three steps: magnetic labelling, magnetic separation and elution of labeled cells (Figure 3.2). After the labelling, cell suspension is applied onto the column and the magnetic field efficiently retains cells labeled with the nano-sized beads.

The flow-through fraction, depleted of the labeled cells, can be collected as the negative fraction, whereas the retained cells can be eluted, removing the column from the separator, as the positively selected cell fraction.

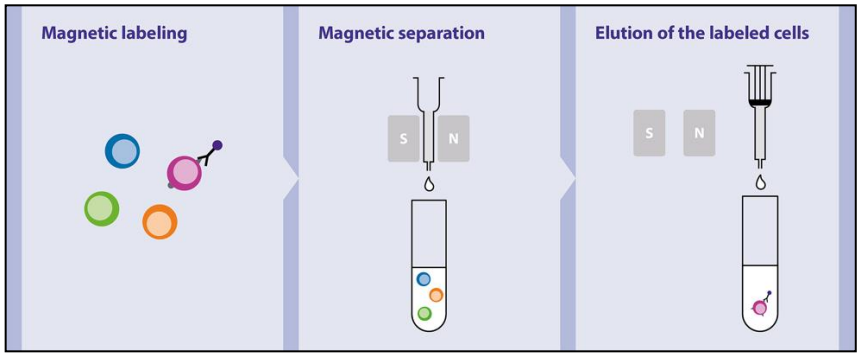

Figure 3.2. Schematic representation of cell separation with MACS® MicroBeads and columns.

3.3.2. Sorting

$CD57^+$ T-LGLs were sorted with the BD FACSAria III cell sorter, which is a specialized flow cytometer with the ability to physically isolate cells of interest into separate collection tubes. The fluidics system of the sorter is responsible for moving particles from the sample injection chamber through the cuvette flow cell for interrogation (Figure 3.3). When a particle is detected and meets the predefined sorting criteria, an electrical charge is applied to the stream just as the droplet containing that particle breaks off from the stream. Then, the charged droplet passes by two strongly charged deflection plates.

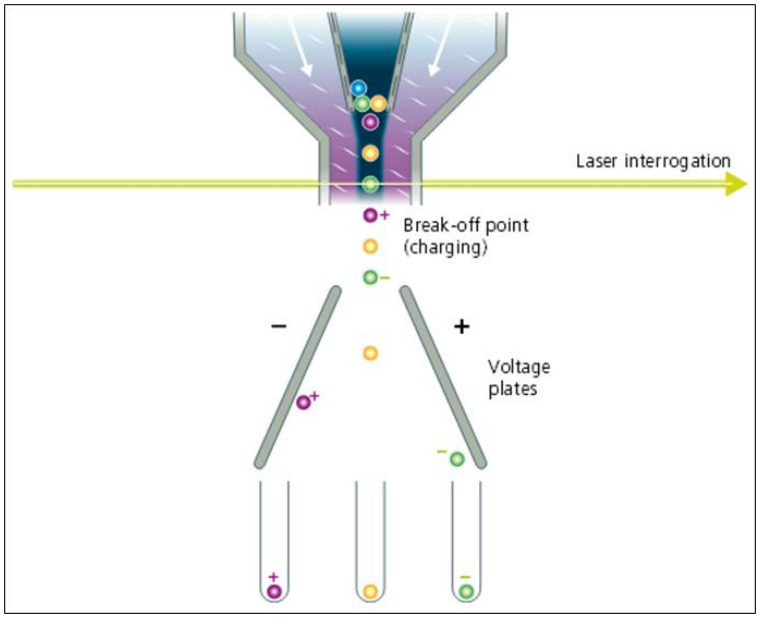

Figure 3.3. Schematic representation of cell sorting process with BD FACSAria™ III cell sorter.

Electrostatic attraction and repulsion cause each charged droplet to be deflected to the left or right, into a collection device, depending on the droplet's charge polarity. Uncharged droplets are not affected by the electric field and pass down the centre to the waste aspirator.

3.4. Flow Cytometry

To characterize the immunophenotype of the leukemic clone and to verify the purity and the viability of the purified populations, samples were analyzed by Flow Cytometry, using a BD FACS CantoII analyzer and the BD FACS Diva software program (BD Biosciences).

3.4.1. Flow Cytometry: principles and application

Flow cytometry provides a multi-parametric analysis of single cells.
A flow cytometer is provided with two detectors: forward scatter (FSC) and side scatter (SSC). The FSC is placed along the incident laser axis and measures the diffracted light, which is related to the cell size; the SSC, instead, is placed at 90° with respect to the incident ray and measures the reflected and refracted light, which is related to the internal complexity of the cell (Figure 3.4).

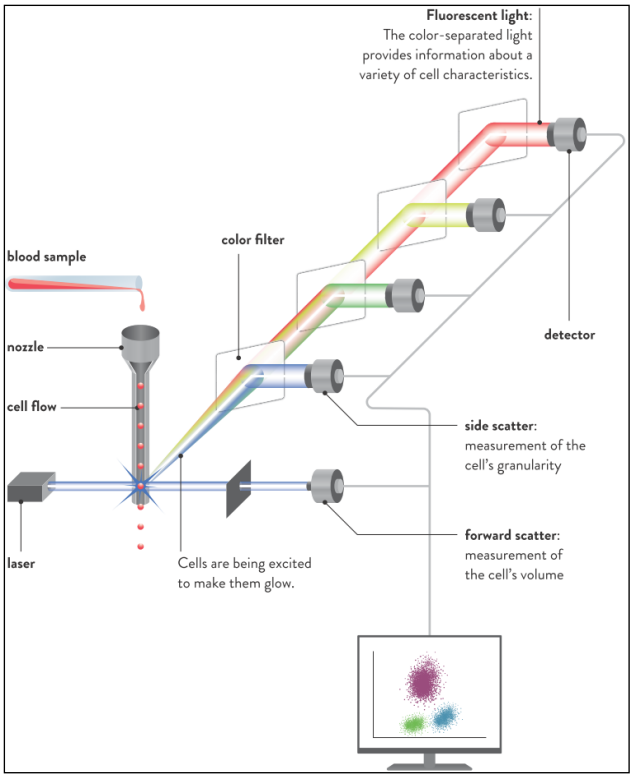

Figure 3.4. Schematic representation of a flow cytometer.

From the contemporary analysis of the FSC and the SSC through a dot plot, it is possible to discriminate different cell populations, based on their morphological features (size and granularity).

Several photomultiplier tubes (one for each type of emitted radiation) amplify the fluorescence signals emitetd by the cell-bound monoclonal antibodies, providing data on the positivity and the level of expression of specific surface markers.

All information is then processed by a software.

3.4.2. Monoclonal antibodies

The immunophenotyping of PBMCs and purified T-LGLs were performed by staining with commercially available mouse monoclonal antibodies (mAbs) (Becton Dickinson, Sunnyvale, CA, USA), reported in Table 3.1.

Antibody	Clone	Fluorescence
anti-CD3	SK7	PE
anti-CD4	SK3	FITC
anti-CD8	RPA-T8	APC
anti-CD16	B73	PE-Cy7
anti-CD56	B159	PE
anti-CD57	NK-1	FITC

Table 3.1. Mouse monoclonal antibodies used in flow cytometry application. FITC: Fluorescein isothiocyanate; PE: Phycoerythrin; APC: Allophycocyanin; PE-Cy7: Phycoerythrin-Cyanine7.

For quantitative determination of the TCR Vβ repertoire of T-LGLs, the IO Test® Beta Mark TCR-Vβ Repertoire kit (Beckman Coulter, CA, USA) was used. The kit consists of 8 vials containing mixture of conjugated TCR Vβ antibodies corresponding to 24 different specificities, covering approximately 70% of the normal human TCR Vβ repertoire.

3.4.3. Annexin V/PI staining

Cell viability was evaluated using the "FITC Annexin V Apoptosis Detection Kit with PI" (Immunostep, Italy).

Apoptosis is a process characterized by a variety of morphological features. One of the earliest indications of apoptosis is the translocation of the membrane phospholipid phosphatidylserine (PS) from the inner to the outer leaflet of the plasma membrane.

Once exposed to the extracellular environment, binding sites on PS become available for Annexin V, which is a 35-36 kDa, Ca^{2+}-dependent, phospholipid binding protein with a high affinity for PS. As such, Annexin V can be conjugated to a fluorochrome, and used for the flow cytometric identification of cells in the early stages of apoptosis.

The loss of membrane integrity, instead, is a process that accompanies the later stages of cell death, resulting from either apoptotic or necrotic processes. Therefore, staining with Annexin V is typically used in conjunction with a vital dye, such as propidium iodide (PI), for identification of early and late apoptotic cells.

Viable cells with intact membranes exclude PI, whereas the membranes of dead and damaged cells are permeable to PI. Therefore, cells that are considered viable are both Annexin V and PI negative, while cells that are in early apoptosis are Annexin V positive and PI negative, and cells that are in late apoptosis or already dead are both Annexin V and PI positive. To asses cell viability of PBMCs or purified LGLs, $0.2x10^6$ cells were washed in PBS to remove medium and resuspended in binding buffer. Annexin V-FITC was added and cells were incubated for 10 minutes at room temperature, in the dark. DNA was stained with PI immediately before proceeding with flow cytometric analysis.

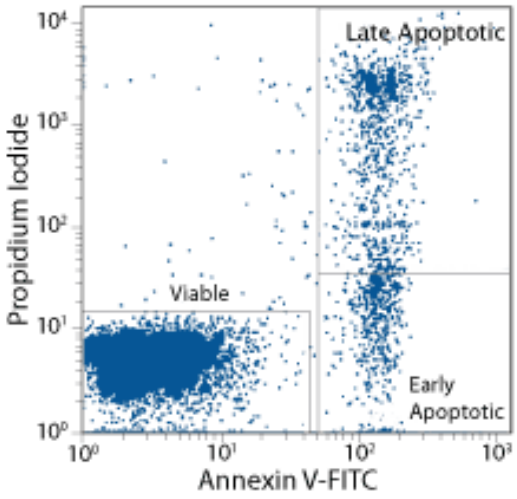

Figure 3.5. Schematic representation of AnnexinV/PI staining.

3.5. Cell cultures

PBMCs or LGLs of patients were cultured in RPMI 1640 medium (EuroClone, Italy) supplemented with: 2nM L-glutamine, 25 mM Hepes, 10% v/v of heated inactivated Fetal Calf Serum, 100 U/ml penicillin and 100 µg/ml streptomycin.

Cells were plated at a final concentration of 2×10^6 cells/ml and were maintained in incubator at 37°C in a modified atmosphere with 5% of CO_2.

The following treatments were employed:

- Stattic (Selleckchem, USA), a STAT3 inhibitor;
- Recombinant Human Interleukin 6 (Sigma-Aldrich, Steinhelm, Germany), a STAT3 ativator.

PBMCs or LGLs were then collected for protein and RNA extraction.

Supernatants were collected and stored at -80°C for ELISA test.

3.6. Proteic analysis

3.6.1. Whole proteins extraction

Freshly isolated cells or cells collected from culture conditions ($0.25x10^6$) were centrifuged at 5000 rpm for 5 minutes. Pellets were resuspended (1:1) in a Sample Buffer, Laemmli 2× Concentrates, which is a solution for denaturing and loading of protein samples in SDS-PAGE, composed of:

- 4% SDS, which denatures the proteins and gives each an overall negative charge;
- 10% 2-mercaptoethanol, which reduces the intra and inter-molecular disulfide bonds;
- 20% glycerol, which increases the density of the sample;
- 0.004% bromphenol blue, which serves as a dye front that runs ahead of the proteins and also serves to make it easier to see the sample during loading;
- 0.125 M Tris HCl, pH 6.8.

Protein samples were heated for 5 minutes at 100°C in in a heat block. Then, they were stored at -20°C for proteic analyses.

3.6.2. SDS-PAGE

Sodium Dodecyl Sulfate Poly-Acrylamide Gel electrophoresis (SDS-PAGE) is an analytical technique to separate SDS-treated proteins, based on their molecular weight. SDS is a detergent with a strong protein-denaturing effect which binds to the protein backbone at a constant molar ratio. In the presence of SDS and a reducing agent that cleaves disulfide bonds, critical for proper folding, proteins unfold into linear chains with negative charge proportional to the polypeptide chain length.

Acrylamide is used to prepare electrophoretic gels suitable for protein separation by size. Acrylamide mixed with bisacrylamide and with the polymerizing agent ammonium persulfate (APS) forms a crosslinked polymer network (polyacrylamide). The polymerization reaction is catalyzes by TEMED (N,N,N,N'-tetramethylenediamine). The size of the pores created in the gel is inversely related to the polyacrylamide percentage (concentration). Low-percentage gels are used to resolve large proteins, and high-percentage gels are used to resolve small proteins. Negative charged denatured proteins, when placed in an electric field, will migrate towards the negative anode inside the poly-acrylamide gel.

The gel typically consists of two sections: a “stacking” gel and a “separating” gel. The stacking gel has a low concentration of acrylamide (5%), that allows the proteins to be concentrated into one tight band before entering the separating gel. An acrylamide concentration between 10 and 15%, instead, was used for separating gel.

Protein samples and a molecular weight reference (Seeblue Plus2 Prestained Standard 1X, Invitrogen) were loaded into different wells in the stacking gel. They were separated using Amersham electrophoretic chambers, a specific saline running buffer (pH 8.3) (25mM Tris, 192mM glycine, 0.1% SDS) and an applied electric field of 25mA (Figure 3.6).

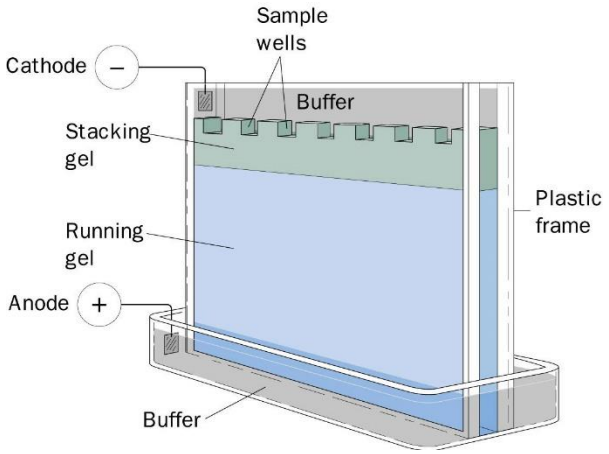

Figure 3.6. Schematic representation of SDS-PAGE technique.

3.6.3. Western Blotting

After the electrophoresis, proteins must be transferred from the electrophoresis gel to a membrane, usually polyvinylidene difluoride (PVDF). In the transfer process voltage is applied to transfer the proteins from the gel to the membrane.

The setup includes sponges, filter papers, the gel, and the membrane, which is placed between the gel and the positive electrode (Figure 3.7). This ensures the migration of the negatively charge proteins from the gel to the membrane. The result is a membrane with a copy of the protein pattern that was originally in the gel.

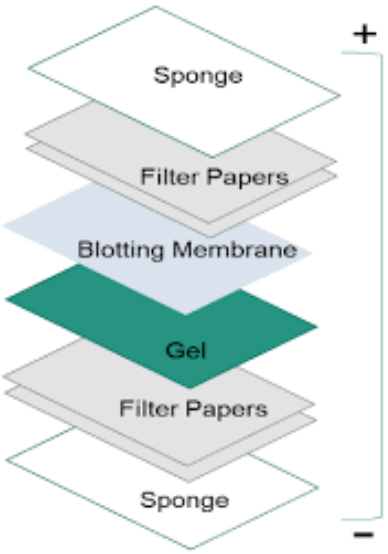

Figure 3.7. Schematic representation of the western blot sandwich.

The transfer is performed in a specific saline buffer containing Tris 250mM, glycine 1.92M and methanol 20%. Since PDVF membrane is highly hydrophobic, it must be pre-wetted with methanol for 1 minute prior to submersion in transfer buffer.

After the transfer, the membrane is saturated to prevent unspecific binding of the detection antibodies during subsequent steps. Saturation is performed for 1 hour in a solution composed of non-fatty milk 5% (Ristora) and TBS (Tris buffered saline) supplemented with Tween-20 0.05% (Sigma). Saturation is followed by washing in TBS plus Tween-20 0.05% in order to remove unbound reagents and reduce the background signal.

The membrane is then incubated overnight at 4°C with a primary antibody that recognizes a specific protein or epitope on a group of proteins. The primary antibody is not directly detectable. Therefore, tagged secondary antibodies that recognize the heavy chains of the primary antibodies are used to detect the target Ag (indirect detection). Secondary antibodies are enzymatically labelled with Horseradish peroxidase. After a final series of washes to remove unattached antibodies, the antibodies on the membranes are ready to be detected.

An appropriate chemiluminescent substrate, which produces light, is then added to the membrane. The light output can be captured using ImageQuant LAS500 machine (GE Healthcare Life Sciences). As chemiluminescent substrates, Pierce ECL western blotting substrate (Thermo Scientific) and LiteAblot PLUS Enhanced Chemiluminescent Substrate (EuroClone) were used.

In order to detect more antibodies with the same specificity and similar molecular weight it is necessary to strip the membrane. Stripping buffer reagent (Thermo scientific) allows the cleaning and the efficient removal of primary and secondary antibodies from immunoblots without removing or damaging the immobilized Ag. This allows blots to be re-probed with new antibodies. Membranes were covered with this buffer and incubated for 20 minutes at 37°C and then washed with TBS, afterwards the membranes were saturated again with milk.

Primary antibodies: anti-phospho-STAT3(Tyr705) (Cell Signaling USA), anti-STAT3 (Cell Signaling USA); anti-β-actin (Cell Signaling, USA);

Secondary antibodies: anti-rabbit IgG HRP-linked antibody (Cell Signaling, USA); HRP labeled goat anti-mouse IgG (KPL, USA).

3.6.4. ELISA test

To quantify sFASL concentration on plasma and supernatant of cell cultures, ELISA test has been used (eBioscience).

The enzyme-linked immunosorbent assay (ELISA) is a tool that provides the quantitative detection of human sFASL present in biological fluids. The principles of the test are based upon the presence of an anti-human sFASL coating antibody that is adsorbed onto microwells, which binds the sFASL present in the sample or standard binds; a biotin-conjugated anti-human sFasL antibody binds to human sFASL captured by the first antibody. Thus, Streptavidin-HRP binds to the biotin conjugated anti-human sFASL. Following incubation, unbound biotin conjugated anti-human sFASL and Streptavidin-HRP are removed through a wash step. Substrate solution reactive with HRP is then added to the wells. The result is the formation of a coloured product in proportion to the amount of soluble human sFASL present in the sample. The reaction is terminated by addition of acid and absorbance is measured at 450nm. A standard curve is prepared from different human sFASL sample, with a known protein concentration.

3.7. Molecular analysis

3.7.1. RNA extraction

RNA was purified using RNeasy® Mini Kit (QIAGEN, Hilden, Germany), according to manufacturer procedures. This procedure combines the selective binding properties of a silica-based membrane with the speed of microspin technology.

Biological samples are first lysed and homogenized in the presence of a highly denaturing guanidine-thiocyanate containing buffer, which inactivates RNases to ensure purification of intact RNA. Ethanol is then added to provide appropriate binding conditions of RNA to the RNeasy membrane. The sample is then applied to the RNeasy® Mini spin column, where RNA binds to the membrane, while contaminants are efficiently washed away. RNA is then eluted in RNase-free water and quantified using the NanoDrop™ 1000 Spectrophotometer (Thermo Scientific) (Figure 3.6).

3.7.2. cDNA synthesis

The reverse transcription from total RNA to complementary DNA (cDNA) was performed using the the Reverse Transcription System (Promega, Madison, WI, USA). The system uses a reverse transcriptase from Avian Myeloblastosis Virus (AMV), with an intrinsic RNase H activity, to synthesize single-stranded cDNA from total or poly(A)+ isolated RNA.

The reaction mixture is composed as indicated in Table 3.2.

Component	**Amount**
$MgCl_2$, 25mM	4 µl
Reverse Transcription 10X Buffer	2 µl
dNTP Mixture, 10mM	2 µl
Recombinant RNasin® Ribonuclease Inhibitor	0.5 µl
AMV Reverse Transcriptase	15 u
Oligo(dT) or Random Primers	0.5 µg
Total RNA	1,5 µg
Nuclease-Free Water to a final volume of	20 µl

Table 3.2. Component of the reaction mixture.

The reverse transcription was performed using a T100™ Thermal Cycler, with the following thermal protocol:

- 42°C for 15 minutes
- 95°C for 5 minutes
- 4°C maintenance

Synthesized cDNA was then stored at -80°C and used for gene expression analyses.

3.7.3. Quantitative Real Time-Polymerase Chain Reaction (qRT-PCR)

The quantitative Real-Time Polymerase Chain Reaction (qRT-PCR) is a method for gene quantification characterized by high sensibility and specificity. It is called "Real-Time PCR" because it allows to observe in real time the increase in the amount of DNA as it is amplified. This is possible because the qRT-PCR system combines a thermal cycler and an optical reaction module that detects and quantifies fluorophores. Molecules added to the PCR mix, as SYBR Green, bind the amplified DNA and emit a signal that increases in proportion to the rise of the amplified DNA products. An amplification curve is obtained, where cycle numbers are found in abscissa and the fluorescence normalized on internal fluorophore in ordinate (Figure 3.7).

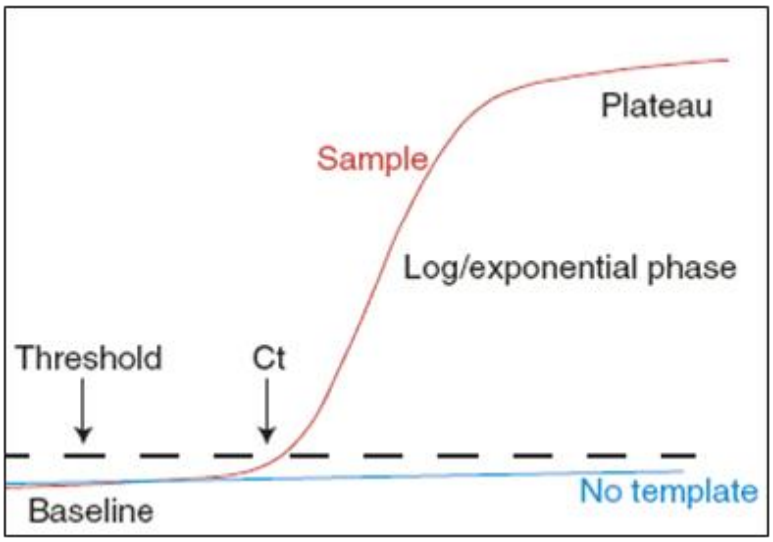

Figure 3.8. Schematic representation of a qRT-PCR reaction.

At the beginning of the reaction there are only little changes in fluorescence and this is the baseline region; the increasing in fluorescence above this threshold underlines amplified product formation. From this point on, the reaction maintains an exponential course that degenerates in plateau at the end of the reaction. In the midway cycles the curve has a linear course: this is the most important phase since the amount of amplified DNA is correlated with the amount of cDNA expressed at the beginning in the sample.

In this linear region a threshold of fluorescence is chosen and from this value it is possible to obtain the Ct (threshold cycle), namely the number of cycles of amplification necessary for the sample to reach that threshold of emission.

SYBR Green was used as detector dye: it emits low fluorescence if present in solution; on the contrary the signal becomes stronger if the dye binds to double strand DNA. However, SYBR Green is not a selective dye and binds to all DNA, even to primer dimers. For this reason, it is recommended the introduction of a further step after amplification, called dissociation protocol. During this step, temperature rises gradually until all the double strands are denatured.

This method allows the identification of contaminants or unspecific amplification products since they show different melting points. Another dye, called ROX, works as an internal reference used by the instrument to normalize the SYBR Green fluorescence.

For the evaluation of gene expression was used a relative quantification method. The original concentration (Co) of each sample was obtained using the following equation: $Co=2^{-\Delta\Delta Ct}$, where:

- ΔCt = Ct (target gene) - Ct (reference gene);
- ΔΔCt = ΔCt (of sample) - ΔCt (of the internal calibrator, which is a sample used as reference and included in every reaction plate to compare different plates' results);
- $2^{-\Delta\Delta Ct}$ (The "2"value represents the higher efficiency for reaction that means a doubling of the product at every cycle of amplification).

The reaction mixture is composed as indicated in Table 3.3.

Component	**Amount**
Roche FastStart Universal SYBR Green Master (ROX)	7.5µl
Forward primer (5µM)	0,9 µl
Reverse primer (5µM)	0,9 µl
H_2O	4.2 µl
cDNA	1.5 µl

Table 3.3. Component of the reaction mixture.

FastStart Taq DNA Polymerase is a hot start polymerase with the following amplification protocol:

- UDG activation 50°C 2 minutes
- Polymerase activation 95°C 10 minutes
- Denaturation 95°C 15 seconds
- Annealing and amplification 60°C 1 minutes

} x 40 cycles

Dissociation protocol: increasing temperature from 60°C to 95°C.

The thermal cycler used was the Sequence Detection System 7000 (Applied Biosystem) and the software was ABI PRISM 7000.

The primer used for amplification of genes of interest were designed by Primer express 3.0 (Applied Biosystems).

Their sequences are reported in Table 3.4.

Gene target	Forward primer	Reverse primer
FasL PT	GCTGCCACCCCTGAAGAAG	CCCTCCATCCCCTTATGCC
FasL mRNA	CCACCCCCTGAAAAAAAGGAG	ATAGGTGTCTTCCCATTCCAG
HuR	TTTGGGCGGATCATCAACTC	ATGGGCTCAGAGGAACCTG
primiR-146b	GAACGGGAGACGATTCACAG	CCTTGGCATTGATGTTGTAGC
GAPDH	AACAGCCTCAAGATCATCAGC	GGATGATGTTCTGGAGAGCC

Table 3.4. Primer sequences designed for qRT-PCR.

3.7.4. DNA extraction

Genomic DNA extraction was performed using "Puregene™ Cell and Tissue" kit (Quiagen).

Purified LGLs are lysed with an anionic detergent in the presence of a DNA stabilizer, that limits the activity DNases. RNA is then removed by treatment with an RNA digesting enzyme. Other contaminants, such as proteins, are removed by salt precipitation. Finally, the genomic DNA is recovered by precipitation with alcohol and dissolved in hydration solution (1 mM EDTA, 10 mM Tris·Cl pH 7.5) (Figure 3.8). Purified DNA typically has an *A*260/*A*280 ratio between 1.7 and 1.9 and is up to 200 kb in size.

DNA was quantified using the NanoDrop™ 1000 Spectrophotometer (Thermo Scientific) and then stored at –20°C, for mutational analyses.

3.7.5. Sanger Sequencing

STATs mutational analysis was performed on purified T-LGLs DNA.

Sanger Sequencing is a multi-step process, consisting of:

- PCR of STAT3 gene exons 20-24 and STAT5b exons 16-17;
- quality control of the amplified products by gel electrophoresis
- purification of the amplified products by agarose gel band cutting
- quality control by agarose gel electrophoresis
- Cycle sequencing, using dye terminator technology
- purification of Cycle-sequencing products using Dye-Ex columns Sanger-Sequencing

In Sanger sequencing, the DNA to be sequenced serves as a template for DNA synthesis. A DNA primer is designed to be a starting point for DNA synthesis on the strand of DNA to be sequenced.

Four individual DNA synthesis reactions are performed. The four reactions include normal A, G, C, and T deoxynucleotide triphosphates (dNTPs), and each contains a low level of one of four dideoxynucleotide triphosphates (ddNTPs): ddATP, ddGTP, ddCTP, or ddTTP. The four reactions can be named A, G, C and T, according to which of the four ddNTPs was included. When a ddNTP is incorporated into a chain of nucleotides, synthesis terminates. This is because the ddNTP molecule lacks a 3' hydroxyl group, which is required to form a link with the next nucleotide in the chain. Since the ddNTPs are randomly incorporated, synthesis terminates at many different positions for each reaction. Following synthesis, the products of the A, G, C, and T reactions are individually loaded into four lanes of a single gel and separated using gel electrophoresis, a method that separates DNA fragments by their sizes. The bands of the gel are detected, and then the sequence is read from the bottom of the gel to the top, including bands in all four lanes. For instance, if the lowest band across all four lanes appears in the A reaction lane, then the first nucleotide in the sequence is A. Then if the next band from bottom to top appears in the T lane, the second nucleotide in the sequence is T, and so on. Due to the use of dideoxynucleotides in the reactions, Sanger sequencing is also called "dideoxy" sequencing.

3.8. miRNA analysis

High throughput and single miRNA analysis were performed in collaboration with Prof. Bazzoni's lab, by using the TaqMan® Human microRNA Array (v3.0, Panels A and B, Applied Biosystems) and the TaqMan® microRNA Human Assays (Applied Biosystems), respectively.

Array data were analysed by Gene Expression Suite software (Applied Biosystems) and Hierarchical Clustering Analysis (HCA) was performed by using Multi Experiment Viewer (MEV). miRNA expression values both from arrays and from single assays were calculated according to the comparative threshold cycle method using U6 as endogenous control. Relative miRNA expressions have been reported as fold change (FC). miRNAs samples with a FC>2 or FC<0.5 and *P*<.05 were considered as differentially expressed as compared to controls.

3.9. Cell transfection

Electroporation is a transfection technology based on the momentary creation of small pores in cell membranes by applying an electrical pulse.

Cell transfection was performed in collaboration with Prof. Bazzoni's lab, in Verona. Jurkat cells (10^6) or freshly purified $CD57^+$ T-LGLs (10^7) were transfected with a miR-146b mimic (ID PM10105, Ambion, Applied Biosystems) or a Scrambled, using the Amaxa Nucleofector™ Technology (Lonza, USA) and the Ingenio Electroporation Solution (Mirus Bio), according to the manufacturer's protocol.

Transfected cells were plated in RPMI 1640 medium (EuroClone, Italy), supplemented as described above, for 24-48 hours before further analysis was done.

3.10. Statistical analysis

Statistical evaluation was performed by using the Mann-Whitney U-test or Student t-test, as appropriate, with α set to 0.05. Correlation coefficient was determined using the Spearman Rank Correlation. P<.05 were considered significant. Hierarchical Clustering Analysis (HCA) of TaqMan Human microRNA Array data was performed by using the Multi Experiment Viewer (MEV, mev.tm4.org/) software with the following parameters: Pearson Correlation and complete linkage.

4. RESULTS

4.1. Characterization of neutropenic T-LGLL patients

4.1.1. Evaluation of neutropenia

In our cohort of 100 T-LGLL patients (50 males, 50 females), neutropenia, defined by an absolute neutrophil count (ANC) lower than 1.5 x 10^9/L, was documented in 39 out of 100 patients (39%). Among these, 17 out of 39 (44%) presented also a severe neutropenia, with an ANC lower than 0.5 x 10^9/L.

4.1.2. Immunophenotypic characterization of T-LGLs of neutropenic patients

In order to define whether neutropenic patients share some phenotypical similarities, by flow cytometry analysis we performed a deep analysis of the immunophenotype of our cohort of patients.

We observed that 68 out of 100 patients (68%) were characterized by $CD3^+/CD8^+/CD4^-$ T-LGLs expansion (defined as $CD8^+$ T-LGLL), while the remaining 32 patients (32%) were characterized by $CD3^+/CD4^+/CD8^{-/dim}$ T-LGLs expansion (defined as $CD4^+$ T-LGLL). According to the expression of CD16, CD56 and CD57, several possible immunophenotypic combinations were demonstrated in both $CD8^+$ and $CD4^+$ T-LGLL group (Figure 4.1).

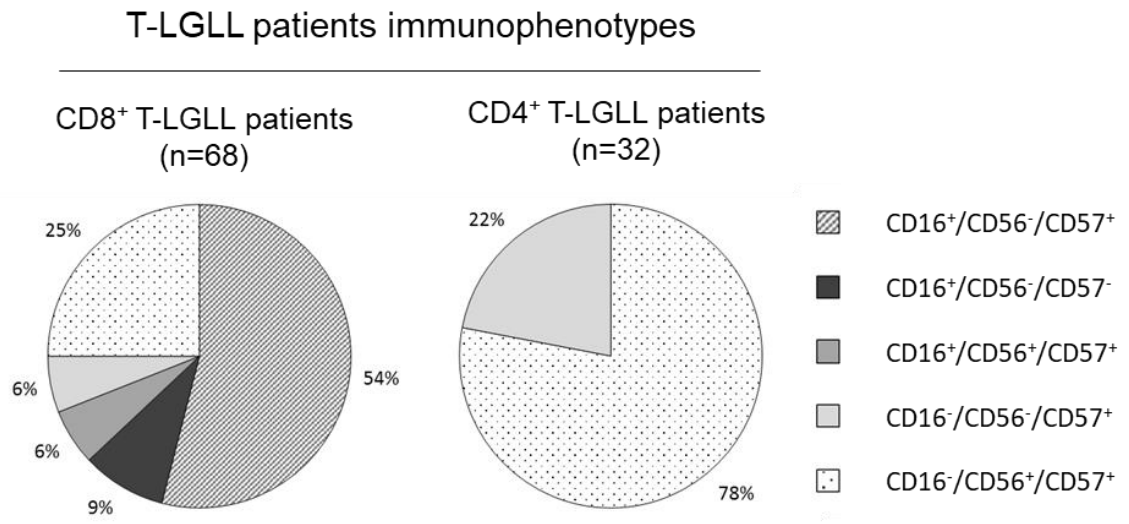

Figure 4.1. Immunophenotypes distribution analysis in T-LGLL patients. The graphs represent the incidence (%) of each immunophenotype in the group of $CD8^+$ T-LGLL patients (pie chart on the left) as compared with the group of $CD4^+$ T-LGLL patients (pie chart on the right).

In $CD8^+$ T-LGLL patients the most common phenotype was $CD16^+/CD56^-/CD57^+$ (37 out of 68, 54%), followed by $CD16^-/CD56^+/CD57^+$ (17 out of 68, 25%), $CD16^-/CD56^-/CD57^+$ (6 out of 68, 9%), $CD16^+/CD56^-/CD57^-$ (4 out of 68, 6%), and $CD16^+/CD56^+/CD57^+$ (4 out of 68, 6%). In $CD4^+$ T-LGLL patients, instead, only two phenotypes were observed: $CD16^-/CD56^+/CD57^+$ (25 out of 32, 78%) and $CD16^+/CD56^+/CD57^+$ (7 out of 32, 22%).

Interestingly, we observed that almost all neutropenic patients (38 out of 39, 97%) belonged to $CD8^+$ T-LGLL subset, while among $CD4^+$ T-LGLL group only one neutropenic patient (1 out of 32, 3%) was found, this last characterized by a mild neutropenia (ANC: 1,47 $x10^9$/L).

Remarkably, we observed that neutropenic patients share also the same CD16, CD56 and CD57 expression pattern, being mainly characterized by $CD8^+/CD16^+/CD56^-/CD57^+$ phenotype (34 out of 39, 87%), followed by $CD8^+/CD16^+/CD56^-/CD57^-$ (3 out of 39, 8%).

In conclusion, the most frequent immunophenotype of neutropenic patients was characterized by the expression of CD8 and CD16 and by the concomitant absence of CD56 (37 patients out of 39, 95%). Only two neutropenic patients (2 out of 39, 5%) showed a different markers expression, being respectively $CD8^+/CD16^-/CD56^-/CD57^+$ and $CD4^+/CD8^{dim}/CD16^+/CD56^+/CD57^+$ (Figure 4.2).

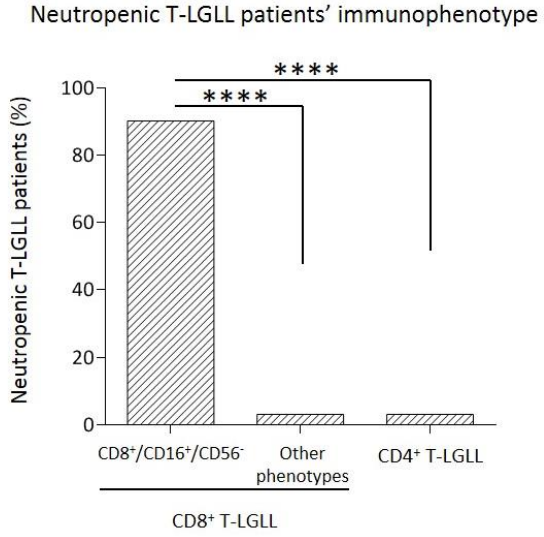

Figure 4.2. Neutropenic patients' immunophenotypes. The histogram represents the percentages of patients with neutropenia (ANC < 1.5 $x10^9$/L) subdivided according to their immunophenotypes. Neutropenia incidence resulted 95% in $CD8^+/CD16^+/CD56^-$ subset and 5% in the other immunophenotypic subsets ($CD8^+$ T-LGLL and $CD4^+$ T-LGLL, respectively). The difference is statistically significant (****P < 0.0001, $\chi^2 = 49.5$ and $\chi^2 = 55.7$, respectively, using χ^2 test).

Differently, the $CD8^+/CD16^+/CD56^-$ immunophenotype was rarely detected both in $CD8^+$ T-LGLL and $CD4^+$ T-LGLL patients with normal ANC (4 out of 61, 7%), proving to be a signature of neutropenic patients.

Consistently, patients included in $CD8^+/CD16^+/CD56^-$ subset showed ANC value significantly lower than that observed in the remaining $CD8^+$ subsets and $CD4^+$ T-LGLL patients (mean ANC ± SEM: 0.795 ± 0.08 $x10^9$/L, 2.86 ± 0.22 $x10^9$/L, 2.6 ± 0.19 $x10^9$/L, respectively, $P<0.05$), confirming that this specific immunophenotype was significantly associated with the presence of neutropenia (Figure 4.3).

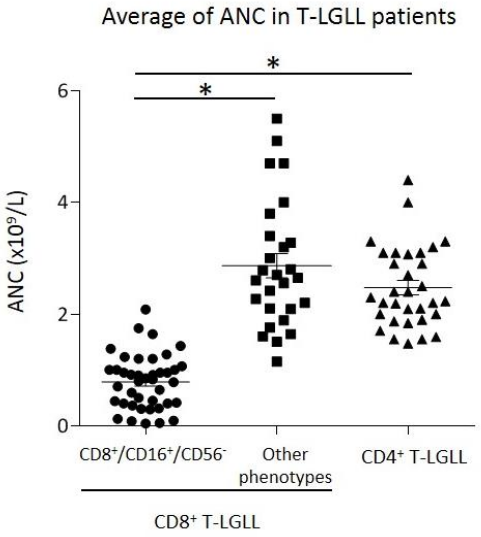

Figure 4.3. ANC evaluation in the patients subdivided according to their immunophenotypes. Dot plot indicating ANC level of each patient. The mean of ANC ± SEM in $CD8^+/CD16^+/CD56^-$ subset (0.795 ± 0.08 $x10^9$/L) is lower than in the other immunophenotypic subsets of $CD8^+$ T-LGLL (2.86 ± 0.22 $x10^9$/L) and in $CD4^+$ T-LGLL (2.6 ± 0.19 $x10^9$/L; *$P < 0.05$, using one-way Anova and Tukey's multiple comparison test).

4.1.3. Evaluation of STATs activation in T-LGLs of neutropenic patients

STAT3 is reported to be constitutively activated in leukemic T-LGLs and to play a pathogenetic role in LGLL. To evaluate whether neutropenic patients were characterized by a major STAT3 transcriptional activity than the other T-LGLL patients, we evaluated STAT3 activation in T-LGLs of our cohort of patients.

We measured, by western blot analysis, STAT3 phosphorylation at $Tyrosine^{705}$ (p-STAT3-Y^{705}) and we observed a high p-STAT3-Y^{705} in T-LGLs obtained by neutropenic T-LGLL patients, belonging to $CD8^+/CD16^+/CD56^-$ subset. Conversely, a lower STAT3 activation was observed in T-LGLs from the other $CD8^+$ subsets with normal ANC or in $CD4^+$ T-LGLs, as compared to $CD8^+/CD16^+/CD56^-$ T-LGLs.

Consistently, the average values, evaluated by densitometric analysis on 26 $CD8^+/CD16^+/CD56^-$ samples, resulted statistically higher as compared with all the other immunophenotypic subsets, evaluated on 23 samples (p-STAT3 Y^{705}/STAT3, median ± SEM: 1.89 ± 0.78 and 0.49 ± 0.10, respectively, $P < 0.01$) (Figure 4.4).

Taken together, our data showed that STAT3 activation clustered with $CD8^+/CD16^+/CD56^-$ phenotype and that neutropenic patients were characterized by higher levels of STAT3 activation as compared to the other T-LGLL patients.

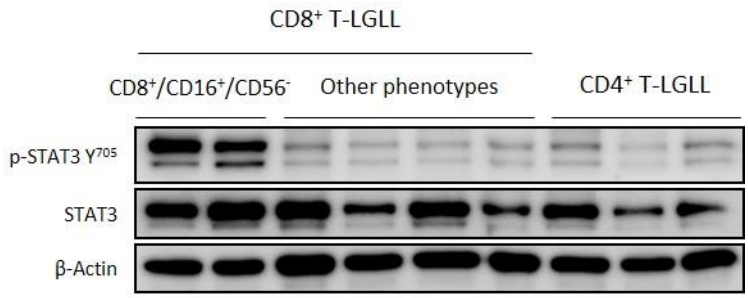

Figure 4.4. Evaluation of STAT3 activation. Western blot analysis on whole-cell extracts (0.25×10^6 $CD57^+$ T-LGLs) purified from representative cases of T-LGLL patients, subdivided according to their different immunophenotypes are reported. Protein levels of p-STAT3-Y^{705} and total STAT3 are reported, β-Actin expression is shown as gel loading control.

To evaluate whether the high levels of STAT3 activation observed in neutropenic patients could be explained by the presence of *STAT3* mutations, we analyzed, by Sanger sequencing, *STAT3* genetic lesions in our cohort of patients.

Our data showed that 38 patients out of 100 analyzed (38%) carried *STAT3* mutations. Among these: 24 cases out of 38 (63,2%) presented Y640F, 9 cases (23,7%) D661Y, one case (2,6%) D661V, one case (2,6%) N647I, one case (2,6%) with a hot spot mutation, K658R, together with an in-frame insertion, I659_M660insL, one case (2,6%) with an in-frame deletion/insertion, A662_N663delinsH, and one case (2,6%) with an in-frame insertion, G656_Y657insY.

We then evaluated the incidence of *STAT3* mutations in our cohort of neutropenic patients. Interestingly, our data showed that almost all neutropenic patients (38 out of 39, 90%) were *STAT3* mutated (Figure 4.5). The correlation between the presence of *STAT3* mutations and neutropenia resulted statistically significant ($\chi^2=63$, $P < 0.001$). Remarkably, all the patients experiencing severe neutropenia were included among the group of mutated cases.

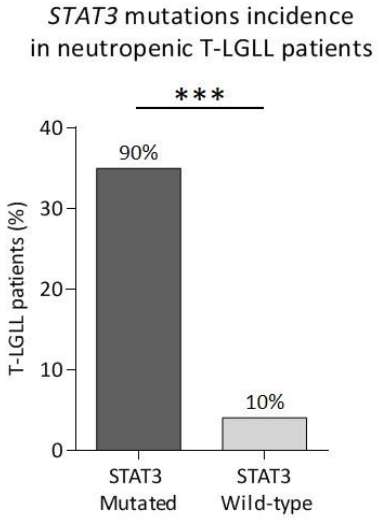

Figure 4.5. Neutropenic patients subdivided depending on the presence/absence of *STAT3* mutations. Among neutropenic patients (n=39), the histogram represents the percentage of patients with *STAT3* mutations (35/39, 90%) and wild type for *STAT3* (4/39, 10%). The difference of neutropenia incidence is statistically significant ($P < .001$).

According to a recent report showing high incidence (55%) of *STAT5b* mutations in CD4+ T-LGLL, we evaluated also the presence of these genetic lesions in our cohort of study. *STAT5b* mutations were found in 5 out of 100 patients (5%) and were represented by N642H (2 out of 5, 40%), Y665F (2 out of 5, 40%) and Q706L (1 out of 5, 20%).

Accordingly to the data reported by Andersson et al., all patients harboring *STAT5b* mutations were affected by $CD4^+$ T-LGLL, even if we observed a lower incidence of these genetic lesions (5 patients out of 32, 16%), as compared to the frequency reported in literature. None of them was neutropenic and neither show any clinical manifestation. Consistently, neutropenic patients did not show different level of STAT5b activation, compared to all the other $CD8^+$ patients (data not shown).

4.1.4. Evaluation of Fas Ligand expression in T-LGLs of neutropenic patients

Soluble FasL, which is increased in the serum of LGLL patients as compared to normal donors, has been hypothesized to play a role in inducing neutropenia.

Therefore, we evaluated FasL expression in our series of patients, subdivided according to their immunophenotype. We analyzed FasL transcriptional expression by Real-Time PCR, showing that it was higher in $CD8^+/CD16^+/CD56^-$ T-LGLL patients as compared to non-neutropenic patients belonging to the other immunophenotypes, both $CD8^+$ and $CD4^+$ T-LGLL (7.66 ± 0.87, 2.45 ± 0.22 and 2.35 ± 0.28 arbitrary units, respectively; $P < 0.001$; Figure 4.6).

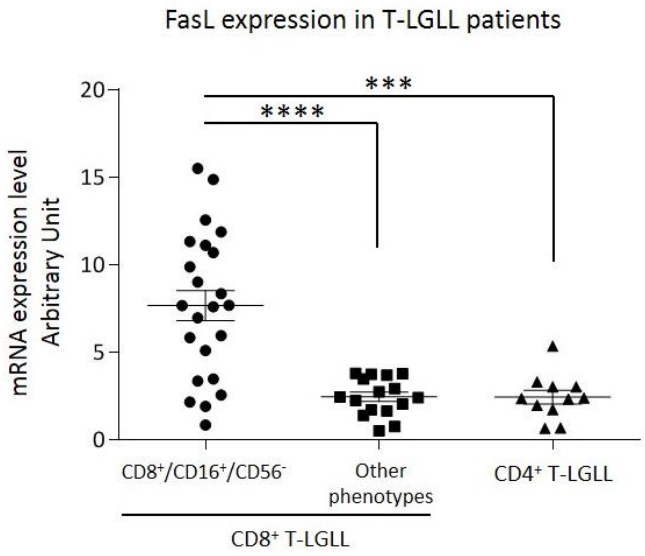

Figure 4.6. Fas ligand expression. Dot plots report Fas ligand mRNA transcription levels of T-LGLL patients subdivided according to their immunophenotypes. The means and SEM are reported. The expression level observed in the group of $CD8^+/CD16^+/CD56^-$ subset is higher as compared with the two other groups (***P < 0.001, ****P < 0.0001, using one-way Anova and Tukey's multiple comparison test).

The difference in FasL production, observed on transcriptional levels, was also confirmed by ELISA test, at protein levels, measuring sFasL level in patients' plasma ($CD8^+/CD16^+/CD56^-$ T-LGLL: 88.3 ± 14.18 pg/ml, the other $CD8^+$ and $CD4^+$ immunophenotypes: 16.08 ± 14.62 pg/ml, P < 0.0001; Figure 4.7).

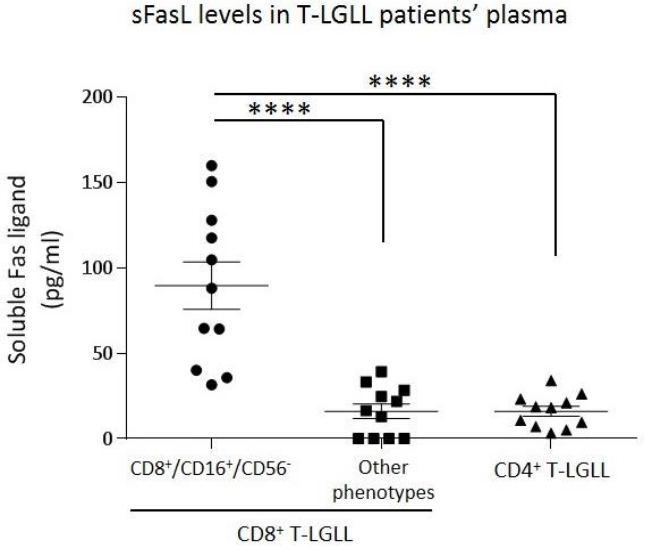

Figure 4.7. Fas ligand expression. Dot plots report secreted Fas ligand plasma levels of T-LGLL patients subdivided according to their immunophenotypes. The means and SEM are reported. The expression level observed in the group of $CD8^+/CD16^+/CD56^-$ subset is higher as compared with the two other groups (***P < 0.001, ****P < 0.0001, using one-way Anova and Tukey's multiple comparison test).

4.1.5. Molecular mechanisms involved in the regulation of Fas Ligand expression

STAT3 is a transcription factor that promotes the expression of thousands of protein-coding genes. To evaluate whether the high level of FasL transcription, observed in neutropenic patients, could depend on STAT3 activation, we inhibited with Stattic (a specific inhibitor of STAT3) or we triggered, with IL-6 (a key cytokine in LGLL development), STAT3 transcriptional activity.

Our data showed that both p-STAT3-Y^{705} and FasL mRNA expression slightly decreased after 2 hours treatment with Stattic (15 µM), as compared to the untreated conditions. On the contrary, when we triggered STAT3 activation with IL-6 (20 ng/ml), we observed, after 1 hour, an increase of p-STAT3-Y^{705}, followed by an increase of 1.59-fold in Fas ligand transcription levels (Figure 4.8).

To verify whether Fas ligand expression was modulated just by STAT3 activation, we pre-treated patients' PBMC for 1 hour with Stattic, before IL-6 incubation. Our data showed that Stattic was able to block IL-6 effect, by preventing p-STAT3-Y^{705} induction and, consequently, to prevent the increase in FasL transcription, both in STAT3 mutated and wild type patients. Therefore, we proved that STAT3 activation plays a crucial role in the regulation of FasL expression.

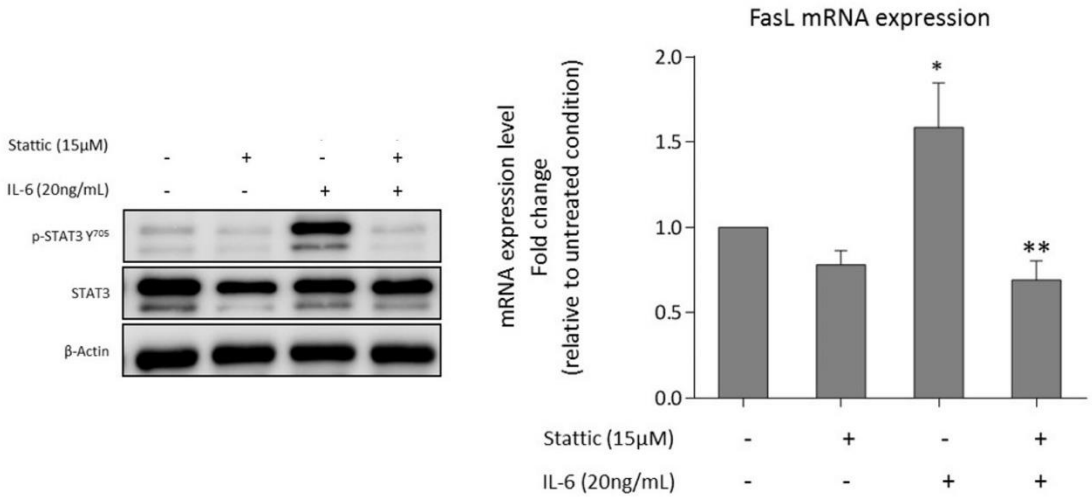

Figure 4.8. FasL regulation. Western blot analysis and Real-Time PCR analysis of one representative out of six independent experiments are shown. Patient's PBMC were cultured in the following different conditions: untreated condition (UT) for 2 hours; with Stattic (15 µM) for 2 hours; stimulated by IL-6 (20 ng/ml) for 1 hour; pretreated for 1 hour with Stattic and then stimulated by IL-6 for 1 hour. On the top, protein levels of p-STAT3-Y^{705} and total STAT3 are reported, β-Actin expression is shown as gel loading control. The histogram on the bottom reports the average fold change of FasL mRNA levels. All the values were settled on untreated condition set at 1.0. Data are represented as mean ± SEM of six independent experiments. *$P < 0.05$ vs. UT; **$P < 0.01$ vs. IL-6 condition, using one-way Anova and Tukey's multiple comparison test.

4.2. Characterization of neutropenic CLPD-NK patients

4.2.1. Evaluation of neutropenia

To characterized NK cells of neutropenic CLPD-NK patients, we performed the same studies in a cohort of 25 CLPD-NK patients. Neutropenia was detected in 10 out of 25 patients (40%), with 5 patients out of 10 (50%) presenting severe neutropenia.

4.2.2. Immunophenotypic characterization of NK cells of neutropenic patients

By flow analysis, NK cells of patients were analysed for CD16 and CD56 expression, defining two major NK cells subsets, *i.e.* patients with $CD56^{dim}/CD16^{dim}$ NK cells (4 out of 25, 16%) and patients with $CD56^{-/dim}/CD16^{high}$ NK cells (21 out of 25, 84%). Almost all neutropenic patients (8 out of 10, 80%) were included in $CD56^{-/dim}/CD16^{high}$ subgroup. Considering the clinical heterogeneity of the $CD56^{-/dim}/CD16^{high}$ subset, we then analysed the expression of CD57 on the cells of these patients, distinguishing two subgroups: patients characterized by a "cytotoxic" phenotype, defined by CD57 negativity, and patients characterized by a "NK memory" phenotype, defined by CD57 positive expression.

Remarkably, all the patients who have experienced severe neutropenia presented a significantly lower CD57 mean expression as compared to the other $CD56^{-/dim}/CD16^{high}$ patients (12.48% ± 2.87 vs 60.43% ± 4.38, $p<0.0001$) (Figure 4.9).

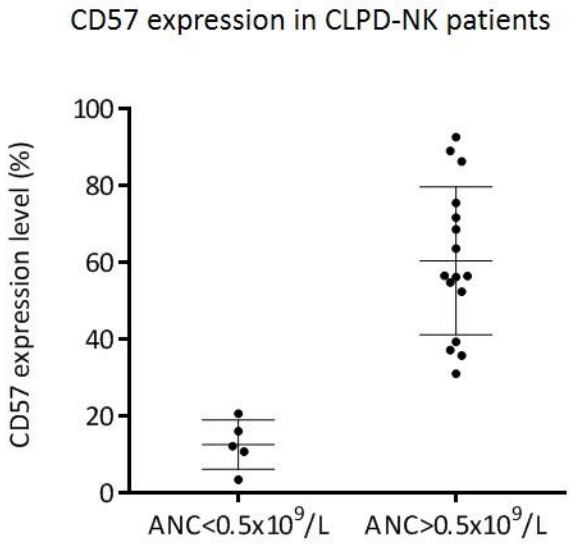

Figure 4.9. CD57 expression levels. Dot plot indicating differential CD57 expression (%) in $CD56^{dim/neg}/CD16^{high}$ subgroup between patients who experienced severe neutropenia (ANC < 0.5 $x10^9$/L) and patients who did not (ANC > 0.5 $x10^9$/L). As represented, patients with ANC < 0.5 $x10^9$/L presented CD57% expression significantly lower ($p < 0.0001$) toward patients with ANC > 0.5 $x10^9$/L.

4.2.3. Evaluation of STATs activation in NK cells of neutropenic patients

We evaluated STAT3 activation in NK cells of our cohort of patients, but, differently from neutropenic T-LGLL patients, we observed a heterogeneous pattern of p-STAT3-Y^{705} among our group of study (data not shown), with only 2 out of 25 patients (8%) harboring *STAT3* mutations.

Moreover, none of them harbored *STAT5b* mutations and we observed a heterogeneous level of STAT5b activation (data not shown).

4.2.4. Evaluation of Fas Ligand expression in NK cells of neutropenic patients

In leukemic T-LGLs, we demonstrated that FasL has a role in the development of neutropenia. Therefore, we analyzed, by Real-Time PCR, FasL transcriptional expression in NK cells of our cohort of patients.

Herein, the heterogeneity revealed in STAT3 activation levels was observed also in FasL expression (Figure 4.10). Therefore, our data, even if they were collected in a small cohort, do not demonstrate a clear role of FasL in neutropenia development in CLPD-NK patients.

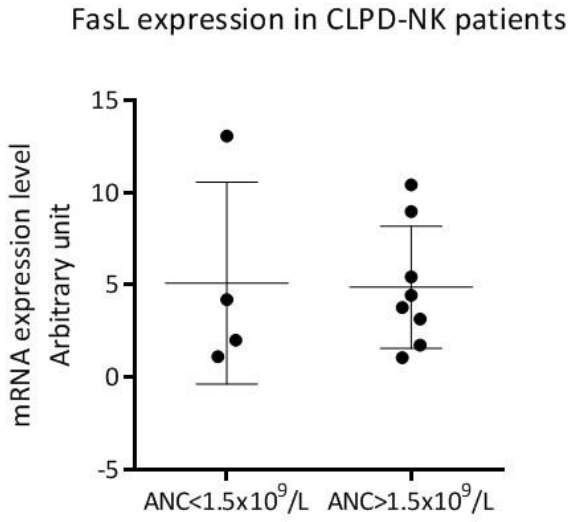

Figure 4.10. Fas ligand expression. Dot plot reports FasL transcription levels of CLPD-NK patients subdivided according to ANC values. The means and SEM are reported. The difference between the expression level observed in the two subsets is not statistically significant ($P > 0.5$).

4.3. Micro-RNA analysis

4.3.1. Characterization of T-LGLs miRNome

We demonstrated that the high levels of FasL detected in neutropenic T-LGLL patients were due to the high STAT3 activation that characterized the T-LGLs of these patients. However, the mechanism through which STAT3 regulates FasL production has not been clarified. Since many microRNAs (miRNAs) are regarded as important gene expression regulators, often involved in the pathogenesis of cancer, we investigated whether the increased FasL production was due to an altered expression of miRNAs.

The miRNAs pattern of expression was investigated in a pilot cohort of patients, using Taq-Man Human microRNA Array. We assessed the expression of 756 mature miRNAs in $CD57^+$ cells purified from 4 neutropenic $CD8^+/CD16^+/CD56^-$ T-LGLL patients, as compared to $CD57^+$ cells purified from 2 $CD4^+$ T-LGLL patients with normal ANC (Table 4.1) and 3 healthy donors (HD).

Patient ID	T-LGLL	T-LGLs phenotype	ANC ($x10^9$/L)	STAT3
LGL 1	$CD8^+$	$CD3^+/CD8^+/CD16^+/CD56^-/CD57^+$	0.95	Mut (Y640F)
LGL 3	$CD8^+$	$CD3^+/CD8^+/CD16^+/CD56^-/CD57^+$	1.43	WT
LGL 5	$CD8^+$	$CD3^+/CD8^+/CD16^+/CD56^-/CD57^+$	1.10	Mut (Y640F)
LGL 9	$CD8^+$	$CD3^+/CD8^+/CD16^+/CD56^-/CD57^+$	0.80	Mut (Y640F)
LGL 10	$CD4^+$	$CD3^+/CD4^+/CD8^-/CD16^+/CD56^+/CD57^+$	5.70	WT
LGL 17	$CD4^+$	$CD3^+/CD4^+/CD8^-/CD16^+/CD56^+/CD57^+$	2.29	WT

Table 4.1. Biological and clinical features of T-LGLL patients studied. ANC: absolute neutrophil count; MUT: mutated; STAT3: Signal Transducer and Activator of Transcription 3; T-LGLL: T-large granular lymphocytes leukaemia; WT: wild type.

Unsupervised Hierarchical Clustering Analysis (HCA) of normalized array data led to the identification of two clusters: cluster A, including the 4 neutropenic $CD8^+$ T-LGLL patients (LGL 1, LGL 3, LGL 5 and LGL 9), and cluster B, including $CD4^+$ T-LGLL patients (LGL 10, LGL 17) together with the 3 HD (HD1, HD2, HD4) (Figure 4.11).

To confirm our previous observation, we evaluated STAT3 activation in whole-cell extracts obtained from $CD57^+$ cells of patients and we observed that a STAT3 activation-dependent/$CD8^+$-specific miRNAs expression pattern was in place (Figure 4.12).

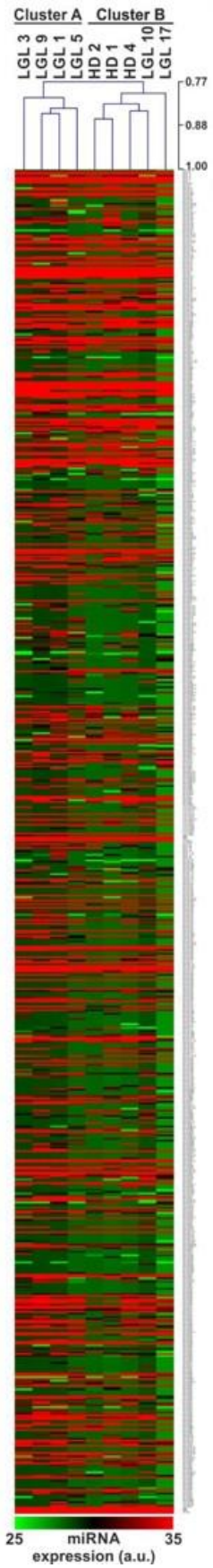

Figure 4.11. miRNome of T-LGLL patients. Heatmap representation of the 756 miRNAs analyzed. Results are expressed as arbitrary units (au) using U6 as reference control.

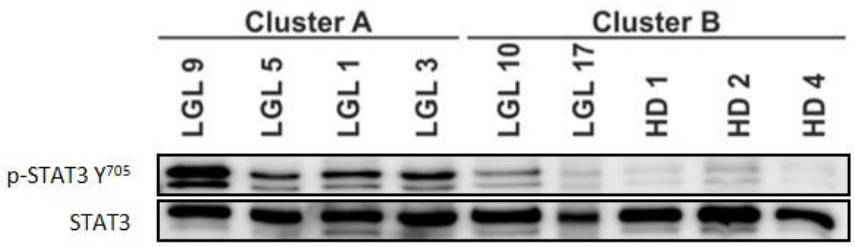

Figure 4.12. miRNome of T-LGLL patients correlates with STAT3 activation. Western blot analysis on whole-cell extracts (250×10^3 $CD57^+$ T-LGLs) purified from the same cells as in Figure 4.10 were loaded on gels and immunoblots were performed. Protein levels of p-STAT3-Y^{705} and total STAT3 are reported.

4.3.2. $CD8^+$ T-LGLs-specific miRNAs expression pattern

We showed that $CD8^+/CD16^+/CD56^-$ T-LGLs expansion is often associated with neutropenia development. Therefore, to investigate whether microRNA could have a role in the pathogenesis of this cytopenia, we studied miRNAs differentially expressed in patients characterized by neutropenia as compared to patients with normal ANC.

First of all, to get insights into the $CD8^+$-specific miRNome, miRNAs expressed in $CD8^+$ and $CD4^+$ T-LGLs have undergone to differential expression analysis. miRNAs showing Ct value <32, and FC value >2 or <0.5 were considered as differentially modulated (Figure 4.13).

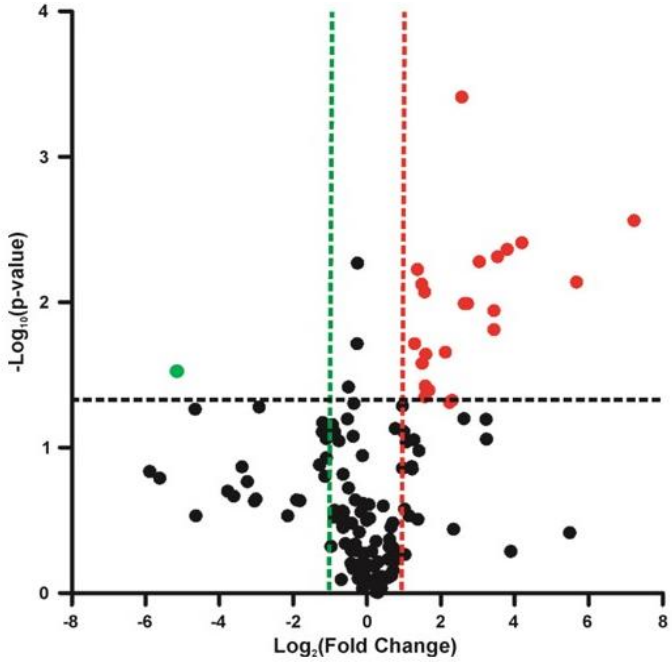

Figure 4.13. miRNAs differentially expressed in CD8 *vs* CD4 T-LGLs. Volcano plot showing miRNAs differentially expressed in CD8 as compared to CD4 T-LGLs. For each miRNA the $-Log_{10}$ (*P* value) is plotted against the average Log_2 (Fold Change). Vertical dashed lines represent the 0.5 and 2 boundary values for the Fold Change (FC), whereas the horizontal dashed line represents the .05 *P* value boundary.

Accordingly, twenty-four miRNAs emerged as up-regulated and only one miRNA, namely miR-146b, as down-regulated in a statistically significant manner (P<.05) in $CD8^+$ as compared to $CD4^+$ T-LGLs (Figure 4.14).

UP-REGULATED		
miRNA	FC	*P*
hsa-miR-501	150.621	.030
hsa-miR-1249	50.970	.007
hsa-miR-1303	18.288	.004
hsa-miR-1227	13.830	.004
hsa-miR-571	11.546	.005
hsa-miR-335#	10.839	.015
hsa-miR-566	10.807	.011
hsa-miR-1247	8.215	.005
hsa-miR-1285	6.586	.010
hsa-miR-33a#	6.194	.010
hsa-miR-591	5.927	.000
hsa-miR-623	4.937	.047
hsa-miR-636	4.719	.049
hsa-miR-625#	4.350	.022
hsa-miR-1267	3.198	.040
hsa-miR-516-3p	3.015	.039
hsa-miR-1253	3.002	.023
hsa-miR-197	2.993	.038
hsa-miR-331-5p	2.970	.045
hsa-miR-1233	2.946	.008
hsa-miR-1825	2.808	.026
hsa-miR-484	2.796	.008
hsa-miR-630	2.572	.006
hsa-miR-939	2.445	.019

DOWN-REGULATED		
miRNA	FC	*P*
hsa-miR-146b	0.028	.030

Figure 4.14. miRNAs differentially expressed in CD8 *vs* CD4 T-LGLs. List of the 25 miRNAs significantly modulated: in green the down-regulated miRNA, in red the up-regulated miRNAs. FC and *P* by unpaired *t*-test are shown FC= fold change.

4.3.3. Correlation analysis of miRNAs expression with ANC and STAT3 activation

MiRNAs selected as differentially expressed in $CD8^+$ and $CD4^+$ T-LGLs were subsequently analyzed for correlation with the absolute neutrophil count (ANC) and STAT3 activation. Correlation analysis highlighted only two miRNAs, namely miR-630 and miR-146b, whose expression correlated with the absolute neutrophil counts (p= -0.886, P=.033 and p=0.866, P=.030, respectively) and simultaneously with the levels of p-STAT3 Y^{705} (p=1.00, P=.003 and p=-0.866, P=.033, respectively) (Table 4.2).

None of the remaining differentially modulated miRNAs correlated with the absolute neutrophil count of patients in a statistically significant manner.

	ANC		STAT3-YP	
	p	P	p	P
hsa-miR-630	**-0.866**	**.030**	**1.000**	**.003**
hsa-miR-146b	**0.866**	**.030**	**-0.866**	**.033**
hsa-miR-939	-0.829	.058	**0.943**	**.017**
hsa-miR-33a#	-0.829	.058	**0.943**	**.017**
hsa-miR-636	-0.829	.080	**0.943**	**.017**
hsa-miR-1285	-0.657	.173	0.829	.058
hsa-miR-1303	-0.600	.242	0.829	.058
hsa-miR-623	-0.600	.242	0.829	.058
hsa-miR-516-3p	-0.543	.297	0.771	.103
hsa-miR-566	-0.543	.297	0.771	.103
hsa-miR-1233	-0.543	.297	0.771	.103
hsa-miR-1247	-0.829	.059	0.657	.175
hsa-miR-1267	-0.600	.240	0.657	.175
hsa-miR-591	-0.543	.297	0.657	.175
hsa-miR-1249	-0.600	.242	0.600	.242
hsa-miR-484	-0.429	.419	0.600	.242
hsa-miR-331-5p	-0.429	.419	0.600	.242
hsa-miR-197	-0.429	.419	0.600	.242
hsa-miR-335#	-0.486	.356	0.543	.297
hsa-miR-571	-0.429	.419	0.543	.297
hsa-miR-625#	-0.486	.356	0.486	.356
hsa-miR-1253	-0.486	.356	0.486	.356
hsa-miR-1825	-0.371	.497	0.486	.356
hsa-miR-501	-0.600	.242	0.429	.419
hsa-miR-1227	-0.429	.419	0.429	.419

Table 4.2. Correlation analysis of miRNA expression, Absolute Neutrophil Count and p-STAT3 Y^{705}. Significant correlations (*P*<.05) are in bold. ANC: absolute neutrophil count; STAT3-YP: Signal Transducer and Activator of Transcription 3 phosphorylated at Tyr705.

4.3.4. Validation analysis on miR-146b

To validate the data collected in our pilot cohort, we performed a RT-qPCR single assay on T-LGLs purified from ad additional cohort of T-LGLL patients, confirming the downregulation of miR-146b expression in $CD8^+$ T-LGLs, as compared to $CD4^+$ T-LGLs (*P*<0.05) (Figure 4.15).

Accordingly, a strong correlation between the expression of miR-146b and ANC (*p*=0.732, *P*=.002) (Figure 4.16) was demonstrated also in the validation cohort. Conversely, miR-630 was confirmed as differentially expressed in $CD4^+$ T-LGLs as compared to $CD8^+$ T-LGLs, but the correlation with ANC was not validated (data not shown).

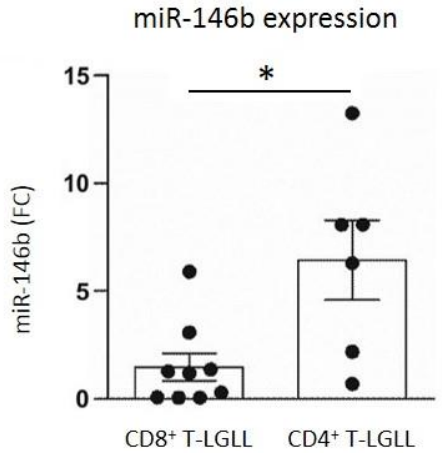

Figure 4.15. miR-146b is differentially expressed in CD8⁺ *vs* CD4⁺ T-LGLs. miR-146b expression in each CD8⁺ and CD4⁺ T-LGLs together with mean ± SEM are shown. * *P*<.05.

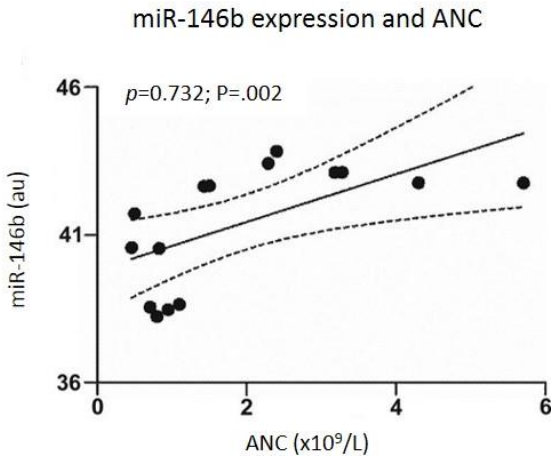

Figure 4.16. Correlation analysis between miR-146b expression and ANC. miR-146b expression is reported as arbitrary units (au); ANCs are reported as cell*10^9/L. Spearman correlation coefficient (*p*) and *P* are reported. * *P*<.05 by Mann-Whitney *U*-test.

4.3.5. Functional characterization of miR-146b

To investigate miR-146b role in neutropenia development, we studied its effects on FasL expression. First of all, by RT-qPCR analysis, we evaluated FasL transcriptional expression in T-LGLs of patients belonging to the validation cohort. According to our previous findings, we found that FasL mRNA expression was higher in neutropenic CD8⁺ T-LGLL patients (mean normalized expression 0.0306 ±0.0067) as compared to the non-neutropenic patients belonging to the CD4⁺ T-LGLL subset (mean normalized expression, MNE: 0.0119 ± 0.0026, *P*=.02).

Remarkably, no difference in the level of FasL primary transcript (FasL-PT) expression between CD8⁺ and CD4⁺ T-LGLs was observed (Figure 4.17).

This new evidence strongly suggested that a post-transcriptional mechanism controlling FasL expression was defective in $CD8^+$ T-LGLL subset, resulting in increased FasL mRNA level. Taken together, these data hinted for a role of miR-146b in the regulation of FasL expression.

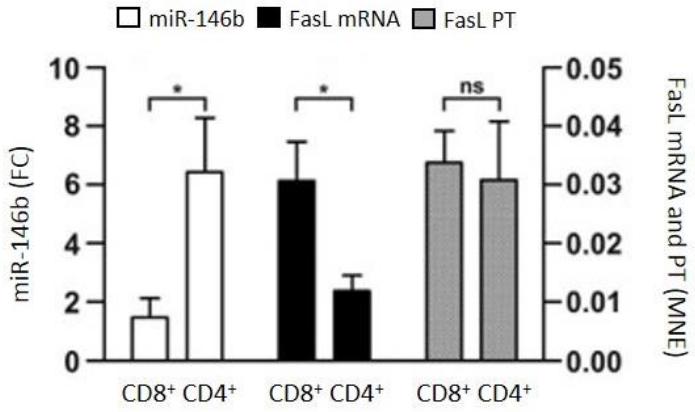

Figure 4.17. miR-146b controls FasL mRNA expression. Correlation between miR-146b and FasL expression in CD8 and CD4 T-LGLs. The expression of miR-146b, FasL mRNA and FasL primary transcript (PT) (A) analyzed in additional $CD8^+$ (n=7) and $CD4^+$ (n=5) T-LGLs by RT-qPCR is reported as mean ± SEM. **P* < .05; ns: not significant by Mann-Whitney *U*-test.

In order verify this hypothesis, Jurkat cells were transfected with a miR-146b mimic. The levels of FasL mRNA expression were then analyzed 48 hours post transfection and our results showed that miR-overexpressing cells had reduced levels of FasL mRNA (MNE $2\times10^{-5} \pm 5.77\times10^{-6}$) as compared to cells transfected with a scramble miRNA control (MNE $3.67\times10^{-5} \pm 6.67\times10^{-6}$) (Figure 4.18). Conversely, restoration of miR-146b expression didn't cause a significant reduction of FasL primary transcript expression.

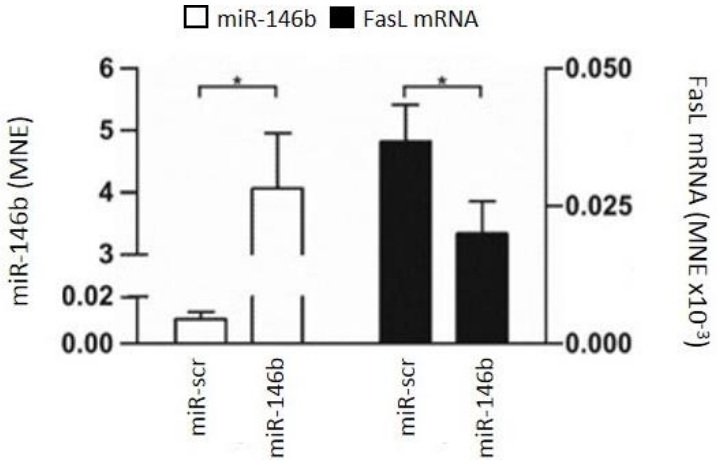

Figure 4.18. Jurkat cells were transfected with 75pmol miR-scr or miR-146b. 48h after transfection cells were processed and miR-146b and FasL mRNA expression were analyzed. Data are expressed as Mean Normalized Expression (MNE) relative to U6 (miR-146b) and GAPDH (FasL mRNA). Mean ± SEM of three independent experiments is shown. * *P*<.05, ns: not significant by paired *t*-test.

We then over-expressed miR-146b in $CD8^+$ T-LGLs purified from patients. The restoration of miR-146b expression in these cells, as observed in the Jurkat cell line, caused a significant reduction of FasL mRNA, but not of primary transcript expression (Figure 4.19).

Collectively, these data demonstrated that the loss of miR-146b was responsible for the increased FasL expression observed in $CD8^+$ T-LGLs, and, consequently, of the related neutropenia.

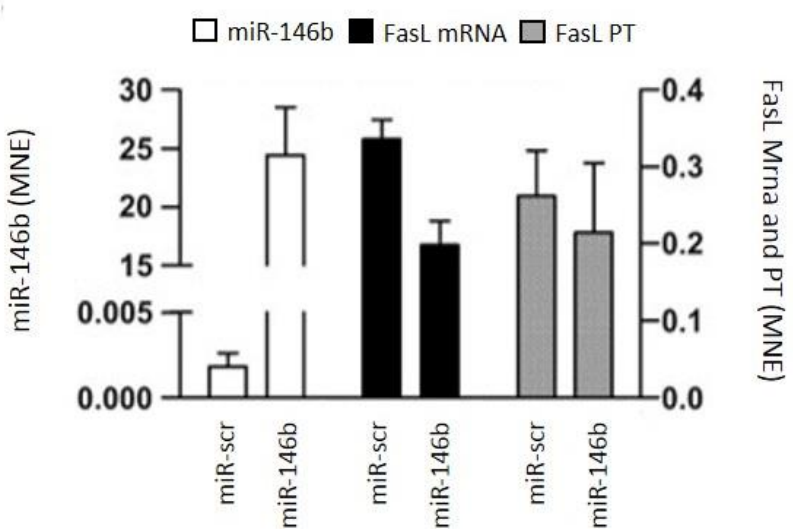

Figure 4.19. CD8 T-LGLs were transfected with 200pmol miR-scr or miR-146b. 24h after transfection cells were processed and miR-146b, FasL mRNA and PT expression were analyzed by RT-qPCR. Data are expressed as MNE relative to U6 (miR-146b) and RPL32 (FasL mRNA and PT). Mean ± SEM of two independent experiments is reported.

4.3.6. HuR is target of miR-146b

To experimentally demonstrate that FASL expression was regulated by miR-146b, i*n silico* miR-target prediction analysis was performed by seven different target prediction software (microT4, miRanda, Pictar2, PITA, RNA22, miRWalk and TargetScan). However, target prediction algoritms did not identify FasL among the miR-146b putative target genes.

Therefore, we supposed that FasL could be an indirect target of this miRNA and we studied wheter FasL transcription factors could be regulated by miR-146b. We found that several FASL transcription factors were predicted as miR-146b putative target genes (Figure 4.20), however we demonstrated that none of these was shown to be regulated by miR-146b (data not shown).

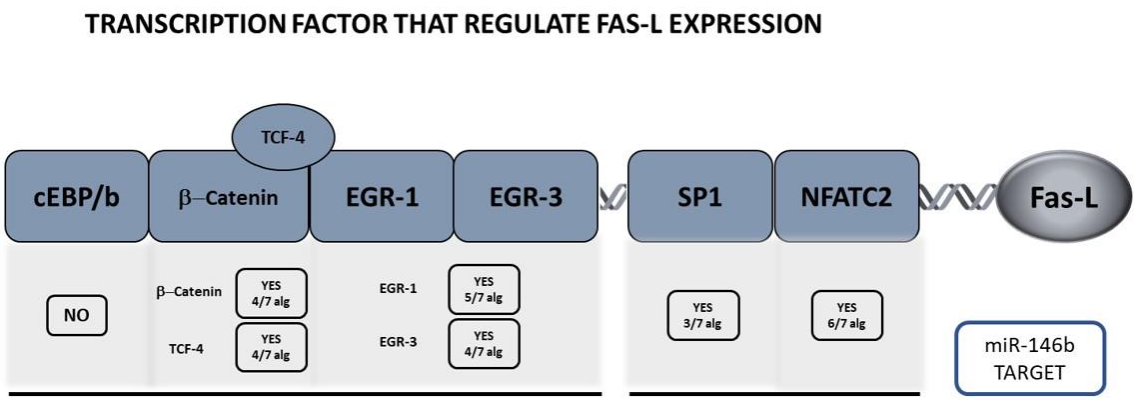

Figure 4.20. FasL transcription factors. Transcription factors that regulate FasL expression and evaluated as putative miR-146b targets.

Thus, we checked for genes involved in FasL mRNA stability. Among the sixteen genes retrieved as putative miR-146b targets, commonly predicted by all softwares, only one, the ribonucleoprotein Human Antigen R (HuR), also known as ELAVL1, play a well-defined role in mRNA stabilization, and has been reported to be absolutely required for FasL expression in T lymphocytes. Moreover, the potential miR-146b binding site in the 3' UTR of HuR (Figure 4.21-A) has been demonstrated to be functional.

HuR mRNA expression levels were reduced in miR-146b overexpressing CD8 T-LGLs (Figure 4.21-B), thus demonstrating that HuR is target of miR-146b.

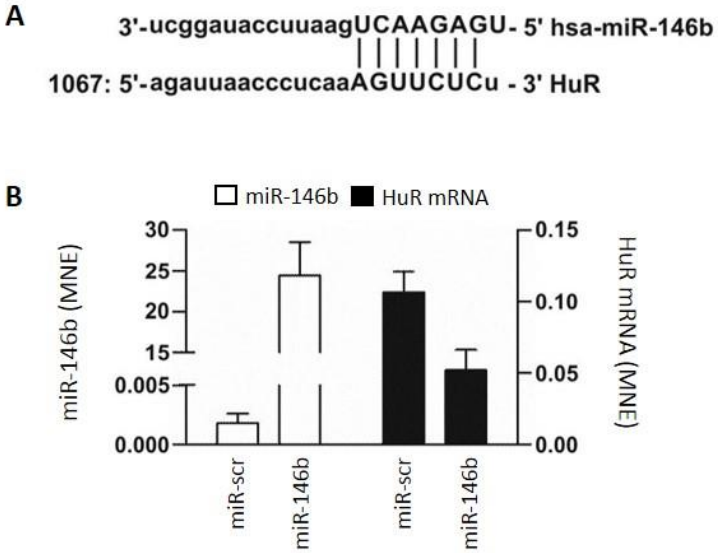

Figure 4.21. (A) Base pairing comparison between mature miR-146b and HuR 3'UTR putative target site is shown according to microRNA.org (http://34.236.212.39/microrna/home.do). (B) CD8 T-LGLs were transfected with 200pmol miR-scr or miR-146b. 24h after transfection cells were processed and miR-146b and HuR mRNA expression were analyzed by RT-qPCR. Data are expressed as MNE relative to U6 (miR-146b) and RPL32 (FasL mRNA and PT). Mean ± SEM of two independent experiments is reported.

4.3.7. Evaluation of HuR expression

To confirm that HuR protein expression inversely correlates with the levels of endogenous miR-146b expression, we evaluated the intracellular levels of HuR protein in $CD8^+$ T-LGLs as compared to $CD4^+$ T-LGLs (Figure 4.21). Remarkably, endogenous HuR protein was detected in $CD8^+$ T-LGLs at levels significantly higher (*P*=.003) than those detected in miR-146b-expressing $CD4^+$ T-LGLs. Collectively, these data show that the lack of miR-146b unleashes the translation of HuR protein, that, in turn, stabilizes FasL mRNA leading to increased FasL production.

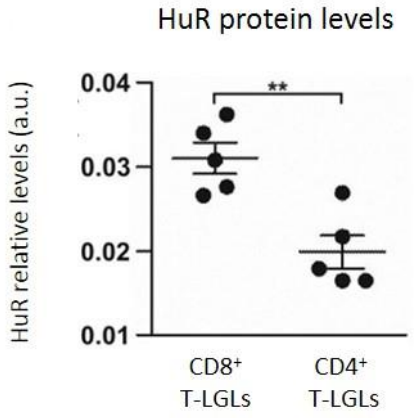

Figure 4.22. HuR protein levels. The relative HuR protein levels, normalized for β-Actin, are reported as arbitrary units (au) below the Western blot. Mean ± SEM is shown (n=3), * *P*<.01 by unpaired *t*-test.

5. DISCUSSION

In a large cohort of T-LGLL patients we showed that the $CD8^+/CD16^+/CD56^-$ immunophenotype and *STAT3* mutations might have a prognostic value for the identification of patients characterized by neutropenia or more susceptible to its development. Moreover, we demonstrated the existence of a miRNA-FasL axis in leukemic T-LGLs, proving the role of miR-146b in neutropenia development through the modulation of FasL expression.

The characterization of neutropenic CLPD-NK patients, instead, showed that they are characterized by $CD56^{-/dim}/CD16^{high}/CD57^-$ cytotoxic NK cells expansion. However, we observed a heterogeneous level of STAT3 activation and a heterogeneous expression of FasL in NK cells this subset of patients.

LGL leukemia, indeed, is a biologically and clinically heterogeneous disease. From a clinical point of view, patients could be asymptomatic at the diagnosis, anyway most of them become symptomatic during the course of the disease. Neutropenia represents the most frequent clinical manifestation and, considering the role of neutrophils in bacterial defence, it represents a negative prognostic factor for patients, since it might lead to recurrent infections. LGLL is usually a clinically indolent disease, thus among all patients, only symptomatic ones require treatments, whereas all the others are usually followed by a *watch-and-wait* approach. For this reason, the identification of a phenotypic and molecular signature of neutropenic patients might become a useful prognostic tool to recognize this high-risk category of patients, who need to be followed with higher frequency than other low-risk patients, since they could develop symptoms related to neutrophils decrease.

First of all, we observed that almost all neutropenic patients were diagnosed with the $CD8^+$ subtype of T-LGLL, while only one patient was characterized by the less frequent $CD4^+$ T-LGLs proliferation. Our data, reporting a normal neutrophil count in $CD4^+$ T-LGLL patients, are consistent with the asymptomatic clinical behavior described for this T-LGLL subtype[55] and address the clinical attention on $CD8^+$ T-LGLL patients. However, not all $CD8^+$ T-LGLL patients became neutropenic: within this T-LGLL category, indeed, different immunophenotypic subset could be recognized, based on the expression of T-

LGLs surface markers. Remarkably, we demonstrated that the presence of neutropenia was mainly, but not exclusively, associated with the $CD8^+/CD16^+/CD56^-$ pattern of markers expression. Thus, our results show that already at diagnosis, the phenotypic analysis of leukemic clone might give information to identify patients who need further investigations.

Our data showed that also *STATs* mutations could represent distinctive molecular features of neutropenic patients. These are the most distinctive genetic lesions described so far in this disease and represent a molecular marker with high specificity, although not exclusive, of LGLs lymphoproliferative disorders. *STATs* mutations do not affect all patients, but only a part of them and, differently from other hematological malignancies (*i.e. BRAF* mutations in Hairy Cell Leukemia), their clinical significance in T-LGLL patients has not been clarified yet. In the literature, has been reported a correlation between the presence of *STAT3* mutations and a more symptomatic disease, particularly with neutropenia [50,58], but these data were not confirmed by other authors. *STAT5b* mutations, instead, are reported to have different clinical impacts, depending on the immunophenotype of the mutated clone: they represent a signature of aggressive clinical course with a poor prognosis in $CD8^+$ T-LGLL patients, while they are devoid of negative prognostic significance in $CD4^+$ T-LGLL patients.

Herein, we demonstrated that neutropenic patients were characterized by a high incidence of *STAT3* mutations, as compared to other phenotypic subsets. Only one neutropenic patient, characterized by $CD4^+$ T-LGLs proliferation, was devoid of STAT3 mutation. STAT5b mutations, instead, were exclusively found in $CD4^+$ T-LGLL patients, accordingly to data reported by Andersson et al. [55], moreover none of the *STAT5b* mutated patients was neutropenic, neither showed any clinical manifestation. Taken together, our findings suggest that the mutational status of the leukemic clone might be taken in account for the characterization of neutropenic patients and, more specifically, that *STAT3* mutational analysis is highly recommended in $CD8^+/CD16^+/CD56^-$ patients. On the contrary, STAT5b mutational analysis do not represent a prognostic marker to identify patients susceptible to neutropenia development and is recommended only in patients with $CD3^+/CD8^+/CD56^+$ phenotype, characterized by an aggressive subtype of T-LGLs proliferation.

Interestingly, our results contribute also to clearly separate $CD4^+$ from $CD8^+$ T-LGLs proliferations, accordingly to the different biological features, that we described in this work, characterizing these subtypes of T-LGLL.

Consistent with the finding that *STATs* mutations promote the phosphorylation of STATs proteins, we observed high p-STAT3-Y^{705} in all neutropenic patients, suggesting that a strong STAT3 activation might represent another specific hallmark of this particular subset.

To bridge the molecular features of neutropenic patients to the clinic, we then pointed our attention on the molecular mechanism of neutropenia development. The pathogenesis of this cytopenia, indeed, still needs to be established. Literature data suggest that it could be multifactorial, comprising both humoral and cytotoxic mechanisms [59]. One of the most relevant hypotheses might be the deregulated expression of FasL by leukemic LGLs, since normal neutrophil survival is partly regulated by the Fas-FasL apoptotic system [31]. Consistently, Liu et al. showed that neutropenia in LGL leukemia patients was consequent to the high level of soluble Fas ligand (sFasL) released by leukemic LGLs, likely responsible to trigger neutrophils apoptosis through Fas receptor.

Here, we provide evidence that sFasL was specifically higher in neutropenic patients, as compared to other subsets and we demonstrated that FasL transcription was mediated by STAT3 activation, explaining why FasL was found to be more expressed in $CD8^+/CD16^+/CD56^-$ patients, who are specifically characterized by higher level of p-STAT3-Y^{705}.

It is well known that FasL expression depends on post-transcriptional events. Important regulators of post-transcriptional modifications are microRNAs, that are small non-coding RNA molecules able to bind target mRNAs, promoting their degradation or blocking protein translation [57]. Furthermore, microRNAs are often involved in the pathogenesis of a variety of conditions, such as cancer and autoimmunity. For instance, STAT3 directly activates miR-21, which is one of microRNAs with a role in promoting cancer cells survival and proliferation.

Interesting insights come from the comparative analysis of the differentially expressed miRNAs within different T-LGLL subsets. The correlation analysis of miRNAs expression pattern with ANC of patients highlighted a strong and significant inverse correlation

between miR-146b expression and neutropenia. Consistently, miR-146b was found to be inversely correlated also with FasL expression. The restoration of the expression of this specific miRNA resulted in a significant reduction of the FasL mRNA expression level, which occurs in the absence of modification of the FasL primary transcript expression. Collectively, these data indicate that miR-146b affects FasL expression at a post-transcriptional level. Nevertheless, *in silico* miR-target prediction analysis did not identify FasL among the putative miR-146b target genes, thus suggesting that miR-146b eventually affects FasL expression indirectly, by targeting genes involved in FasL mRNA stability. In fact, we demonstrated that the intracellular mRNA level of HuR (one of the sixteen genes retrieved as putative miR-146b targets independently predicted by seven miRNA-target prediction software) is affected by miR-146b over-expression. HuR, a ubiquitously expressed member of the HuR family of RNA-binding proteins, has a known role in mRNA stabilization and has been reported to be associated to the ARE-containing 3'UTR of FasL mRNA, which is mandatory for its expression[60]. Remarkably, HuR has been experimentally validated as miR-146b target genes in glioma stem cells and endothelial cells, and the predicted miR-146b seed region located in the 3'UTR of HuR mRNA has been demonstrated to be functional. According to these published data, restoration of miR-146b expression in patients $CD8^+$ T-LGLs decreases the levels of HuR mRNA and, consistently, of FasL. Noticeably, a statistically significant difference in the levels of endogenous HuR protein between $CD8^+$ and $CD4^+$ T-LGLs is detectable.

Thus, by the evaluation of a relevant number of miRNAs, we identified a correlation between the miRNAs expression profile and individual T-LGLs population, characterized by a specific phenotype and by high levels of constitutive STAT3 phosphorylation. Our results, therefore, point to STAT3 activation as the most relevant factor, that drives the expression of CD8-specific miRNAs, in the pathogenesis of neutropenia. The pathogenetic mechanism that we propose is schematically represented in Figure 5.1.

Further studies need to be performed to demonstrate the pathogenetic link between STAT3 activation and miR-146b defective expression. One hypothesis we are going to evaluate points to an epigenetic silencing of miR-146b promoter, mediated by STAT3, as reported in some neoplastic conditions[61,62]. Indeed, it was demonstrated that STAT3 directly induces the expression of the DNA (Cytosine-5)-methyltransferase 1 (DNMT1)

in malignant T-cells and several studies have reported the central role of this enzyme in promoting DNA methylation and, thus, epigenetic gene silencing in cancer.

Therefore, our future perspectives are the study of the methylation of miR-146b promoter and of the analysis of DNMT1 expression in these patients.

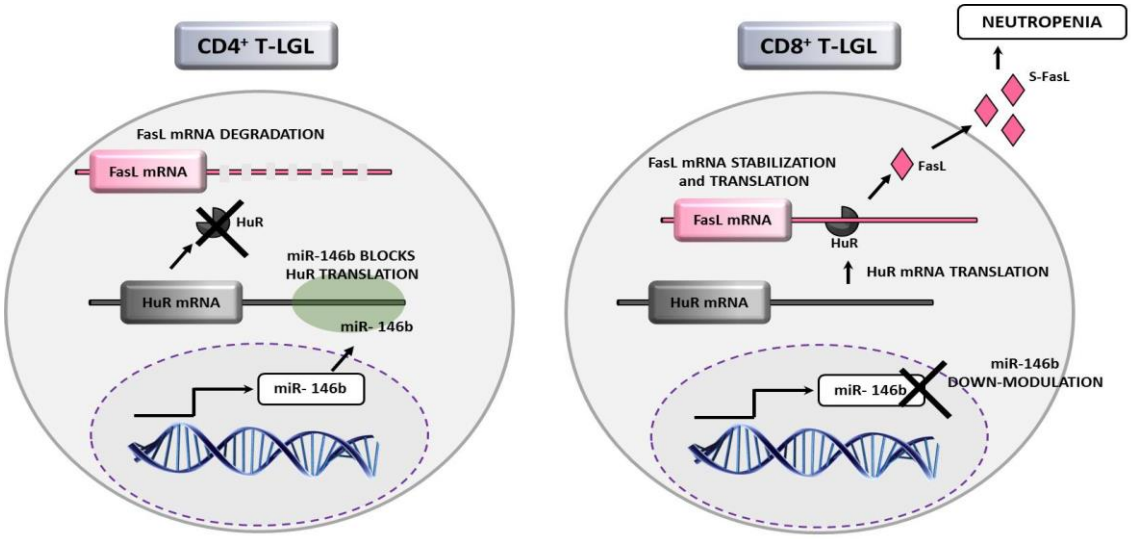

Figure 5.1. Schematic representation of the molecular mechanism accounting for neutropenia development in T-LGLL patients. T-LGL: T-Large Granular Lymphocyte; FasL: Fas Ligand; sFasL: soluble Fas Ligand; HuR:Human Antigen R;

In CLPD-NK, instead, the characterization of neutropenic patients highlighted that they represent a subset with distinctive feature, *i.e.* characterized by $CD56^{-/dim}/CD16^{high}/CD57^{-}$ cytotoxic NK cells expansion. However, the heterogeneous level of STATs activation and the very low incidence of *STATs* mutations observed in these patients lead to hypothesise that different molecular mechanisms might play a role in neutropenia development in CLPD-NK. One of our future perspectives is the whole exome sequencing of NK cells of CLPD-NK patients, to identify new potential genetic lesions that might have a pathogenetic role also in neutropenia development.

Thus, our results confirmed that CLPD-NK and T-LGLL are biologically different diseases and so further studies will be carried out to understand the pathogenetic mechanisms leading to neutropenia development also in these patients.

In conclusion, this study, performed in a large cohort of patients, provides evidence for a link between biological markers (phenotype, *STAT3* mutations and activation, FasL production) and neutropenia, confirming also the well-known heterogeneity of LGLL.

Moreover, our data emphasize the relevance of flow cytometry and STAT3 mutation analysis to gain information on clinical course of disease.

In addition, our extensive evaluation of miRNA landscape in T-LGLL patients indicates that miRNAs are likely involved in sustaining T-LGLs proliferation by contributing to amplify the signal along activating pathways involved in the pathogenesis of LGLL. Remarkably, for the first time the current study demonstrates a direct role of miR-146b in the development of neutropenia reported in a subset of LGLL patients, representing a potential target for individualized therapeutic approaches.

6. REFERENCES

1. Semenzato G, Zambello R, Starkebaum G, Oshimi K, Loughran TP, Jr. (1997) The lymphoproliferative disease of granular lymphocytes: updated criteria for diagnosis. Blood 89: 256-260.
2. Wlodarski MW, Schade AE, Maciejewski JP (2006) T-large granular lymphocyte leukemia: current molecular concepts. Hematology 11: 245-256.
3. Zambello R, Semenzato G (1998) Large granular lymphocytosis. Haematologica 83: 936-942.
4. Loughran TP, Jr. (1993) Clonal diseases of large granular lymphocytes. Blood 82: 1-14.
5. Sokol L, Loughran TP, Jr. (2006) Large granular lymphocyte leukemia. Oncologist 11: 263-273.
6. Shah MV, Zhang R, Loughran TP, Jr. (2009) Never say die: survival signaling in large granular lymphocyte leukemia. Clin Lymphoma Myeloma 9 Suppl 3: S244-253.
7. Loughran TP, Jr., Kadin ME, Starkebaum G, Abkowitz JL, Clark EA, et al. (1985) Leukemia of large granular lymphocytes: association with clonal chromosomal abnormalities and autoimmune neutropenia, thrombocytopenia, and hemolytic anemia. Ann Intern Med 102: 169-175.
8. Swerdlow SH, Campo E, Pileri SA, Harris NL, Stein H, et al. (2016) The 2016 revision of the World Health Organization classification of lymphoid neoplasms. Blood 127: 2375-2390.
9. Jerez A, Clemente MJ, Makishima H, Koskela H, Leblanc F, et al. (2012) STAT3 mutations unify the pathogenesis of chronic lymphoproliferative disorders of NK cells and T-cell large granular lymphocyte leukemia. Blood 120: 3048-3057.
10. Suzuki R, Suzumiya J, Nakamura S, Aoki S, Notoya A, et al. (2004) Aggressive natural killer-cell leukemia revisited: large granular lymphocyte leukemia of cytotoxic NK cells. Leukemia 18: 763-770.
11. Lamy T, Moignet A, Loughran TP, Jr. (2017) LGL leukemia: from pathogenesis to treatment. Blood 129: 1082-1094.
12. Moignet A, Lamy T (2018) Latest Advances in the Diagnosis and Treatment of Large Granular Lymphocytic Leukemia. Am Soc Clin Oncol Educ Book: 616-625.
13. Imamura N, Kuramoto A (1988) Effect of splenectomy in aggressive large granular lymphocyte leukaemia. Br J Haematol 69: 577-578.
14. Gabrielli S, Ortolani C, Del Zotto G, Luchetti F, Canonico B, et al. (2016) The Memories of NK Cells: Innate-Adaptive Immune Intrinsic Crosstalk. J Immunol Res 2016: 1376595.
15. Garrido P, Ruiz-Cabello F, Barcena P, Sandberg Y, Canton J, et al. (2007) Monoclonal TCR-Vbeta13.1+/CD4+/NKa+/CD8-/+dim T-LGL lymphocytosis: evidence for an antigen-driven chronic T-cell stimulation origin. Blood 109: 4890-4898.
16. Zambello R, Trentin L, Facco M, Cerutti A, Sancetta R, et al. (1995) Analysis of the T cell receptor in the lymphoproliferative disease of granular lymphocytes: superantigen activation of clonal CD3+ granular lymphocytes. Cancer Res 55: 6140-6145.
17. Zambello R, Semenzato G (2009) Large granular lymphocyte disorders: new etiopathogenetic clues as a rationale for innovative therapeutic approaches. Haematologica 94: 1341-1345.
18. Zhang D, Loughran TP, Jr. (2012) Large granular lymphocytic leukemia: molecular pathogenesis, clinical manifestations, and treatment. Hematology Am Soc Hematol Educ Program 2012: 652-659.
19. Lamy T, Loughran TP, Jr. (2003) Clinical features of large granular lymphocyte leukemia. Semin Hematol 40: 185-195.
20. Sanikommu SR, Clemente MJ, Chomczynski P, Afable MG, 2nd, Jerez A, et al. (2018) Clinical features and treatment outcomes in large granular lymphocytic leukemia (LGLL). Leuk Lymphoma 59: 416-422.
21. Zhang R, Shah MV, Loughran TP, Jr. (2010) The root of many evils: indolent large granular lymphocyte leukaemia and associated disorders. Hematol Oncol 28: 105-117.

22. Viny AD, Lichtin A, Pohlman B, Loughran T, Maciejewski J (2008) Chronic B-cell dyscrasias are an important clinical feature of T-LGL leukemia. Leuk Lymphoma 49: 932-938.
23. Burks EJ, Loughran TP, Jr. (2006) Pathogenesis of neutropenia in large granular lymphocyte leukemia and Felty syndrome. Blood Rev 20: 245-266.
24. Evans HL, Burks E, Viswanatha D, Larson RS (2000) Utility of immunohistochemistry in bone marrow evaluation of T-lineage large granular lymphocyte leukemia. Hum Pathol 31: 1266-1273.
25. Morice WG, Kurtin PJ, Tefferi A, Hanson CA (2002) Distinct bone marrow findings in T-cell granular lymphocytic leukemia revealed by paraffin section immunoperoxidase stains for CD8, TIA-1, and granzyme B. Blood 99: 268-274.
26. Rustagi PK, Han T, Ziolkowski L, Farolino DL, Currie MS, et al. (1987) Granulocyte antibodies in leukaemic chronic lymphoproliferative disorders. Br J Haematol 66: 461-465.
27. Starkebaum G, Martin PJ, Singer JW, Lum LG, Price TH, et al. (1983) Chronic lymphocytosis with neutropenia: evidence for a novel, abnormal T-cell population associated with antibody-mediated neutrophil destruction. Clin Immunol Immunopathol 27: 110-123.
28. Epling-Burnette PK, Painter JS, Chaurasia P, Bai F, Wei S, et al. (2004) Dysregulated NK receptor expression in patients with lymphoproliferative disease of granular lymphocytes. Blood 103: 3431-3439.
29. Lamy T, Liu JH, Landowski TH, Dalton WS, Loughran TP, Jr. (1998) Dysregulation of CD95/CD95 ligand-apoptotic pathway in CD3(+) large granular lymphocyte leukemia. Blood 92: 4771-4777.
30. O'Donnell JA, Kennedy CL, Pellegrini M, Nowell CJ, Zhang JG, et al. (2015) Fas regulates neutrophil lifespan during viral and bacterial infection. J Leukoc Biol 97: 321-326.
31. Liu JH, Wei S, Lamy T, Epling-Burnette PK, Starkebaum G, et al. (2000) Chronic neutropenia mediated by fas ligand. Blood 95: 3219-3222.
32. Papadaki HA, Eliopoulos AG, Kosteas T, Gemetzi C, Damianaki A, et al. (2003) Impaired granulocytopoiesis in patients with chronic idiopathic neutropenia is associated with increased apoptosis of bone marrow myeloid progenitor cells. Blood 101: 2591-2600.
33. Papadaki HA, Stamatopoulos K, Damianaki A, Gemetzi C, Anagnostopoulos A, et al. (2005) Activated T-lymphocytes with myelosuppressive properties in patients with chronic idiopathic neutropenia. Br J Haematol 128: 863-876.
34. Loughran TP, Jr., Zambello R, Ashley R, Guderian J, Pellenz M, et al. (1993) Failure to detect Epstein-Barr virus DNA in peripheral blood mononuclear cells of most patients with large granular lymphocyte leukemia. Blood 81: 2723-2727.
35. Zambello R, Trentin L, Agostini C, Francia di Celle P, Francavilla E, et al. (1993) Persistent polyclonal lymphocytosis in human immunodeficiency virus-1-infected patients. Blood 81: 3015-3021.
36. Sokol L, Agrawal D, Loughran TP, Jr. (2005) Characterization of HTLV envelope seroreactivity in large granular lymphocyte leukemia. Leuk Res 29: 381-387.
37. Zhang R, Shah MV, Yang J, Nyland SB, Liu X, et al. (2008) Network model of survival signaling in large granular lymphocyte leukemia. Proc Natl Acad Sci U S A 105: 16308-16313.
38. Leblanc F, Zhang D, Liu X, Loughran TP (2012) Large granular lymphocyte leukemia: from dysregulated pathways to therapeutic targets. Future Oncol 8: 787-801.
39. Bousoik E, Montazeri Aliabadi H (2018) "Do We Know Jack" About JAK? A Closer Look at JAK/STAT Signaling Pathway. Front Oncol 8: 287.
40. Hammaren HM, Virtanen AT, Raivola J, Silvennoinen O (2018) The regulation of JAKs in cytokine signaling and its breakdown in disease. Cytokine.
41. Arora L, Kumar AP, Arfuso F, Chng WJ, Sethi G (2018) The Role of Signal Transducer and Activator of Transcription 3 (STAT3) and Its Targeted Inhibition in Hematological Malignancies. Cancers (Basel) 10.
42. Shahmarvand N, Nagy A, Shahryari J, Ohgami RS (2018) Mutations in the signal transducer and activator of transcription family of genes in cancer. Cancer Sci 109: 926-933.

43. Takeda K, Akira S (2001) Multi-functional roles of Stat3 revealed by conditional gene targeting. Arch Immunol Ther Exp (Warsz) 49: 279-283.
44. Akira S (2000) Roles of STAT3 defined by tissue-specific gene targeting. Oncogene 19: 2607-2611.
45. Takeda K, Noguchi K, Shi W, Tanaka T, Matsumoto M, et al. (1997) Targeted disruption of the mouse Stat3 gene leads to early embryonic lethality. Proc Natl Acad Sci U S A 94: 3801-3804.
46. Yao Z, Cui Y, Watford WT, Bream JH, Yamaoka K, et al. (2006) Stat5a/b are essential for normal lymphoid development and differentiation. Proc Natl Acad Sci U S A 103: 1000-1005.
47. Teglund S, McKay C, Schuetz E, van Deursen JM, Stravopodis D, et al. (1998) Stat5a and Stat5b proteins have essential and nonessential, or redundant, roles in cytokine responses. Cell 93: 841-850.
48. Moriggl R, Topham DJ, Teglund S, Sexl V, McKay C, et al. (1999) Stat5 is required for IL-2-induced cell cycle progression of peripheral T cells. Immunity 10: 249-259.
49. Epling-Burnette PK, Liu JH, Catlett-Falcone R, Turkson J, Oshiro M, et al. (2001) Inhibition of STAT3 signaling leads to apoptosis of leukemic large granular lymphocytes and decreased Mcl-1 expression. J Clin Invest 107: 351-362.
50. Koskela HL, Eldfors S, Ellonen P, van Adrichem AJ, Kuusanmaki H, et al. (2012) Somatic STAT3 mutations in large granular lymphocytic leukemia. N Engl J Med 366: 1905-1913.
51. Andersson E, Kuusanmaki H, Bortoluzzi S, Lagstrom S, Parsons A, et al. (2016) Activating somatic mutations outside the SH2-domain of STAT3 in LGL leukemia. Leukemia 30: 1204-1208.
52. Dutta A, Yan D, Hutchison RE, Mohi G (2018) STAT3 mutations are not sufficient to induce large granular lymphocytic leukaemia in mice. Br J Haematol 180: 911-915.
53. Teramo A, Gattazzo C, Passeri F, Lico A, Tasca G, et al. (2013) Intrinsic and extrinsic mechanisms contribute to maintain the JAK/STAT pathway aberrantly activated in T-type large granular lymphocyte leukemia. Blood 121: 3843-3854, S3841.
54. Rajala HL, Olson T, Clemente MJ, Lagstrom S, Ellonen P, et al. (2015) The analysis of clonal diversity and therapy responses using STAT3 mutations as a molecular marker in large granular lymphocytic leukemia. Haematologica 100: 91-99.
55. Andersson EI, Tanahashi T, Sekiguchi N, Gasparini VR, Bortoluzzi S, et al. (2016) High incidence of activating STAT5B mutations in CD4-positive T-cell large granular lymphocyte leukemia. Blood 128: 2465-2468.
56. Loughran TP, Jr., Zickl L, Olson TL, Wang V, Zhang D, et al. (2015) Immunosuppressive therapy of LGL leukemia: prospective multicenter phase II study by the Eastern Cooperative Oncology Group (E5998). Leukemia 29: 886-894.
57. Ikeda S, Tagawa H (2014) Dysregulation of microRNAs and their association in the pathogenesis of T-cell lymphoma/leukemias. Int J Hematol 99: 542-552.
58. Qiu ZY, Fan L, Wang L, Qiao C, Wu YJ, et al. (2013) STAT3 mutations are frequent in T-cell large granular lymphocytic leukemia with pure red cell aplasia. J Hematol Oncol 6: 82.
59. Pontikoglou C, Kalpadakis C, Papadaki HA (2011) Pathophysiologic mechanisms and management of neutropenia associated with large granular lymphocytic leukemia. Expert Rev Hematol 4: 317-328.
60. Drury GL, Di Marco S, Dormoy-Raclet V, Desbarats J, Gallouzi IE (2010) FasL expression in activated T lymphocytes involves HuR-mediated stabilization. J Biol Chem 285: 31130-31138.
61. Xiang M, Birkbak NJ, Vafaizadeh V, Walker SR, Yeh JE, et al. (2014) STAT3 induction of miR-146b forms a feedback loop to inhibit the NF-kappaB to IL-6 signaling axis and STAT3-driven cancer phenotypes. Sci Signal 7: ra11.
62. Walker SR, Xiang M, Frank DA (2014) STAT3 Activity and Function in Cancer: Modulation by STAT5 and miR-146b. Cancers (Basel) 6: 958-968.

"…instead of the great number of precepts of which logic is composed, I believed that the four following would prove perfectly sufficient for me, provided I took the firm and unwavering resolution never in a single instance to fail in observing them.

The first was never to accept anything for true which I did not clearly know to be such; that is to say, carefully to avoid precipitancy and prejudice, and to comprise nothing more in my judgement than what was presented to my mind so clearly and distinctly as to exclude all ground of doubt.

The second, to divide each of the difficulties under examination into as many parts as possible, and as might be necessary for its adequate solution.

The third, to conduct my thoughts in such order that, by commencing with objects the simplest and easiest to know, I might ascend by little and little, and, as it were, step by step, to the knowledge of the more complex; assigning in thought a certain order even to those objects which in their own nature do not stand in a relation of antecedence and sequence.

And the last, in every case to make enumerations so complete, and reviews so general, that I might be assured that nothing was omitted".

Rene Descartes,

"Discourse on the Method of Rightly Conducting One's Reason and of Seeking Truth in the Sciences"